Using TiO2 to Optimize the Photocatalytic Degradation of Kraft Black Liquor Using Response Surface Methodology

Zihan Wang
University of Windsor, wang1fz@uwindsor.ca

Using TiO$_2$ to Optimize the Photocatalytic Degradation of Kraft Black Liquor Using

Response Surface Methodology

By

Zihan Wang

A Major Research Paper

Submitted to the Faculty of Graduate Studies

through the Department of Civil and Environmental Engineering

in Partial Fulfillment of the Requirements for

the Degree of Master of Applied Science

at the University of Windsor

Windsor, Ontario, Canada

2019

Using TiO$_2$ to Optimize the Photocatalytic Degradation of Kraft Black Liquor Using Response Surface Methodology

by

Zihan Wang

APPROVED BY:

_____
P. Henshaw
Department of Civil and Environmental Engineering

_____
N. Biswas, Advisor
Department of Civil and Environmental Engineering

August 26, 2019

DECLARATION OF CO-AUTHORSHIP

I. Co-Authorship

I hereby declare that this thesis incorporates material that is result of joint research, as follows: collaboration with Mrs. Christina Jung. The collaboration is covered in Chapter 2 and Chapter 3. In all cases, the experimental designs were discussed with Dr. Nihar Biswas, based on his suggestion and recommendations made, the key ideas, primary contributions, data analysis, interpretation and writing were performed by the author, and the contribution of co-author C. Jung was primarily through the assisting of developing the laboratory methods and techniques.

I am aware of the University of Windsor Senate Policy on Authorship and I certify that I have properly acknowledged the contribution of other researchers to my thesis, and have obtained written permission from the co-author to include the above material in my thesis.

I certify that, with the above qualification, this thesis, and the research to which it refers, is the product of my own work.

II. General

I declare that, to the best of my knowledge, my thesis does not infringe upon anyone's copyright nor violate any proprietary rights and that any ideas, techniques, quotations, or any other material from the work of other people included in my thesis, published or otherwise, are fully acknowledged in accordance with the standard referencing practices. Furthermore, to the extent that I have included copyrighted material that surpasses the

bounds of fair dealing within the meaning of the Canada Copyright Act, I certify that I have obtained a written permission from the copyright owner(s) to include such material(s) in my thesis.

I declare that this is a true copy of my thesis, including any final revisions, as approved by my thesis committee and the Graduate Studies office, and that this thesis has not been submitted for a higher degree to any other University or Institution.

ABSTRACT

The Canadian pulp and paper industry has been concerned with reducing annual emissions of pollutants into water bodies, air and landfills. Black liquor is a major byproduct from pulp mills such as Kraft. Black liquor is utilized in boilers to produce steam and electricity. Black liquor is a low-value chemical and researchers have employed thermal and chemical processes to produce products such as oils, adhesives, and dispersants. In recent years, photocatalysis has become an alternative to degrade black liquor into short chain carbon chemicals.

This study aims to optimize the performance of black liquor photocatalytic degradation using the TiO_2/UV system. Five practical factors were selected to develop the optimal total organic carbon (TOC) reduction. A two-level 2^k design was used as the preliminary study for examining the optimal initial concentration of black liquor and TiO_2. A three-level Box-Behnken design (BBD) with three factors that included pH, temperature, and particle size was then applied to further enhance the photocatalytic performance. The greatest TOC removal of $36.2\pm4.0\%$ after 4 hours UV irradiation was obtained for 230 mg $TS \cdot L^{-1}$ black liquor and 2 g$\cdot L^{-1}$ TiO_2. The black liquor concentration had larger impact on TOC removal in comparison with TiO_2 concentration. A response surface methodology (RSM) model was developed to predict the maximum 4-hour TOC reduction of 51.6% under optimal conditions of a pH of 7.87, 37 °C, and a catalyst particle size of 5 nm. Compared with the preliminary study, an additional improvement of 15% TOC removal efficiency was observed using the BBD.

Keywords: TiO_2/UV photocatalysis, 2^k design, BBD, TOC reduction.

DEDICATION

To the beloved family and anyone who encouraged and supported me a lot during my studies.

ACKNOWLEDGEMENTS

TABLE OF CONTENTS

LIST OF TABLES

LIST OF FIGURES

LIST OF ABBREVIATIONS/SYMBOLS

ACF	Activated carbon fiber
AD	Anderson-Darling
Adj SS	Adjusted sum of squares
ANOVA	Analysis of variance
AOP	Advanced oxidation process
Au	Gold
BBD	Box-Behnken design
e_{CB}^-	Conductive band
$CaCO_3$	Sodium carbonate
CaO	Lime
COD	Chemical oxygen demand
Cu	Copper
DF	Degrees of freedom
DOE	Design of experiment
$e^-\text{-}h^+$	Electron-hole
Fe	Iron
FFD	Full factorial design
Ga	Gallium
HCl	Hydrochloric acid
H_2O	Water
H_3PO_4	Phosphoric acid

IC	Inorganic carbon
Ir	Iridium
LS	Sodium lignosulfonate
MS	Mean square
NaOH	Sodium hydroxide
Na_2S	Sodium sulfide
Na_2CO_3	Sodium carbonate
Nb	Niobium
OFAT	One-factor-at-a-time
OH^-	Hydroxyl ions
Pt	Platinum
RPM	Revolutions per minute
RSM	Response surface methodology
SS	Sum of squares
SSA	Specific surface area
TC	Total carbon
TiO_2	Titanium dioxide
TOC	Total organic carbon
TS	Total solids
UV	Ultraviolet
VS	Volatile solids
h_{VB}^+	Valence band
% w/w	Weight percent

ZnO   Zinc oxide

•OH   Hydroxyl radical

•O$_2^-$ Superoxide anions radical

GENERAL INTRODUCTION

Background

The pulp and paper industry is the second largest contributor to water pollution in Canada [1]. Pollutants in pulp mill liquid effluents include chemicals such as phenols and formic acid are harmful to receiving waters and toxic to aquatic life. A major process stream arising from cooking wood chips with chemicals is black liquor [2]. This stream is characterized with large amounts of inorganic and organic chemicals. Black liquor is a by-product of the Kraft process, a common manufacturing technique that separates cellulose and hemicellulose from lignin. Through the Kraft process, one metric ton of pulp can generate approximately 10 metric tons of weak black liquor [3]. In Canada, over 16 million metric tons of wood pulp were produced annually between 2012 and 2017 [4], including at least 150 million metric tons of black liquor every year.

One of the primary components of black liquor is lignin, which accounts for 35–45% w/w of the dry solids in black liquor [5]. Lignin, also referred to as "nature's glue," is the second of the three most common natural polymers, bonding hemicellulose to cellulose. In nature, lignin deposits in the cell walls of plants results in mechanical strength and oxidation resistance. Lignin can resist chemical and biological degradation with highly branched and aromatic structure, and dark color and recalcitrance of lignin make black liquor very difficult to treat [6]. Moreover, the recalcitrance of lignin is the major cause of residual high levels of remaining chemical oxygen demand (COD) in treated pulp and paper mills wastewaters [7]. To degrade lignin, many methods have been developed, such as hydrothermal liquefaction [8], and electrocoagulation [9]. Photocatalysis, an evolving process, has been employed to deconstruct lignin [10].

Photocatalysis is widely considered an effective solution for the degradation of various organic compounds, including lignin in black liquor [11]. Photocatalysis is classified as an advanced oxidation process (AOP), which can oxidize organic matters into inorganics, water, and carbon dioxide using the strong oxidants produced from the photo-excited semiconductor catalyst. Hence, it is advantageous as photocatalysis is a clean, efficient, and cost-saving technology [12]. Various metal oxides can be employed in the photocatalytic degradation. The photocatalytic properties of these metal oxides are dependent on their band gap, surface area, and stability [13]. Metal oxides, such as those of zinc and titanium, are activated by either visible or UV light, forming electron-hole (e^--h^+) on the surface. Subsequently, these photo-excited pairs produce radicals with a strong oxidation capability. These radicals are able to oxidize a variety of chemicals into harmless byproducts. Photocatalysts such as titanium dioxide (TiO_2) are very active on the nanoscale, but their photocatalytic performance are less effective on the micrometer scale [14]. Apart from particle size, the photocatalytic conversion efficiency is also dependent upon many other process factors, such as reaction temperature, catalyst concentration, and pH [15]. In order to obtain an optimum conversion efficiency, it is necessary to examine the effect of various factors on the photocatalysis process. The impact of various factors on the efficiency of a process can be examined using response surface methodology (RSM). A popular RSM is the Box-Behnken design (BBD). The BBD method is unique because the design is spherical with fewer experiments when compared to a full factorial design (FFD) [16]. Generally, the BBD is regarded as one of the efficient alternative approaches to labor-intensive designs such as the FFD [17].

RSM is one of the optimization techniques that attempt to optimize multiple variables

simultaneously. With the assistance of a collection of statistical and mathematical algorithms, a well-fit polynomial equation can be developed to describe how the experimental variables affect responses. Before RSM can be applied, it is crucial to have reasonable experimental design and adequate measurements of the response. Some experimental design matrices were available for the RSM, such as the Doehlert design, the three-level factorial design as well as the BBD [18]. An appropriate design should be applied based on the pros and cons of each experimental design. As the RSM is completed, a set of optimal parameters will be determined from the response surface generated by the RSM. Furthermore, the analysis of variance (ANOVA), as statistical analysis, can be utilized to assess the statistical significance and relevance of each factor as well as the interaction effects between these factors.

In Chapter 1, the literature review describes the photocatalysis of black liquor through the following five topics: the reactants, photocatalysts, experimental factors, the products, and different optimization methods. In Chapter 2, the related chemicals and experimental instruments are summarized and described.

In Chapter 3, a preliminary experimental approach based on the 2^k factorial design was used to examine the effects of black liquor concentration and TiO_2 concentration on photodegradation. The significant effect of each factor on the photocatalytic efficiency was determined, and the optimal factor values were retained for further studies described in Chapter 4.

In Chapter 4, the primary analysis was performed using a three-factor BBD, involving pH, temperature, and particle size. The RSM model was developed and conducted for the optimal values of these three factors.

Chapter 5 presents the conclusions of this study with recommendations for future work.

References

[1] Government of Canada, National pollutant release inventory (NPRI)-pollutant release data aggregated by province, industry type and substance, five-year tabular format, (2018). https://open.canada.ca/data/en/dataset/ea0dc8ae-d93c-4e24-9f61-946f1736a26f (accessed July 21, 2019).

[2] H. Niemi, J. Lahti, H. Hatakka, S. Kärki, S. Rovio, M. Kallioinen, M. Mänttäri, M. Louhi-Kultanen, Fractionation of organic and inorganic compounds from black liquor by combining membrane separation and crystallization, Chem. Eng. Technol. 34 (2011) 593–598.

[3] H. Tran, E. Vakkilainen, The kraft chemical recovery process, Tappi Press, 2008.

[4] Natural Resources Canada, Statistical data, (2018). https://cfs.nrcan.gc.ca/statsprofile/production-and-investment (accessed July 21, 2019).

[5] C.D. Blasio, S.D. Gisi, A. Molino, M. Simonetti, M. Santarelli, M. Bjorklund-Sankiaho, Concerning operational aspects in supercritical water gasification of kraft black liquor, Renew. Energ. 130 (2019) 891–901.

[6] V.D. Re, L. Papinutti, Black liquor decolorization by selected white-rot fungi, Biotechnol. Appl. Biochem. 165 (2011) 406–415.

[7] I.A. Kerstin, V.P. Andrey, M. Norgren, M. Eriksson, B. Holmbom, Effects of biological treatment on the chemical structure of dissolved lignin-related substances in effluent from thermomechanical pulping, Nord. Pulp. Pap. Res. J. 23 (2008) 164–171.

[8] A. Orebom, J.J. Verendel, J.S.M. Samec, High yields of bio oils from hydrothermal processing of thin black liquor without the use of catalysts or capping agents, ACS Omega 3 (2018) 6757–6763.

[9] N. Rastegarfar, R. Behrooz, N. Bahramifar, Electrocoagulation treatment of black liquor from soda-AQ pulping of wheat straw, Environ. Monit. Assess. 187 (2015) 1–9.

[10] W. Den, V.K. Sharma, M. Lee, G. Nadadur, R.S. Varma, Lignocellulosic biomass transformations via greener oxidative pretreatment processes: Access to energy and value-added chemicals, Front. Chem. 6 (2018) 141.

[11] L. Cai, Q. Long, C. Yin, Synthesis and characterization of high photocatalytic activity and stable Ag_3PO_4/TiO_2 fibers for photocatalytic degradation of black liquor, Appl. Surf. Sci. 319 (2014) 60–67.

[12] S.H. Li, S. Liu, J.C. Colmenares, Y.J. Xu, A sustainable approach for lignin valorization by heterogeneous photocatalysis, Green Chem. 18 (2016) 594–607.

[13] M.M. Khan, S.F. Adil, A. Al-Mayouf, Metal oxides as photocatalysts, J. Saudi. Chem. Soc. 19 (2015) 462–464.

[14] T.L. Hathway, Titanium dioxide particle size effects on the degradation of organic molecules, in: W. Jenks, R. Larock, H. Stauffer (Eds.), Thesis, Lowa State University, 2007.

[15] K.M. Reza, A. Kurny, F. Gulshan, Parameters affecting the photocatalytic degradation of dyes using TiO_2: A review, Appl. Water Sci. 7 (2017) 1569–1578.

[16] S.L.C. Ferreira, R.E. Bruns, H.S. Ferreira, G.D. Matos, J.M. David, G.C. Brandao, E.G.P. Silva, L.A. Portugal, P.S. Reis, A.S. Souza, W.N.L. Santos, Box-Behnken design: An alternative for the optimization of analytical methods, Anal. Chim. Acta 597 (2007) 179–186.

[17] G. Ye, L. Ma, L. Li, J. Liu, S. Yuan, G. Huang, Application of Box-Behnken design and response surface methodology for modeling and optimization of batch flotation of coal, Int. J. Coal. Prep. Util. (2017) 1–15.

[18] M.A. Bezerra, R.E. Santelli, E.P. Oliveira, L.S. Villar, L.A. Escaleira, Response surface methodology (RSM) as a tool for optimization in analytical chemistry, Talanta 76 (2008) 965–977.

CHAPTER 1

LITERATURE REVIEW

1.1. Introduction

1.1.1. The Kraft process

The Kraft process is a chemical pulping process which was first applied in a pulp mill of Sweden in 1890. The process later became the dominant method of wood cooking in the 1930s after G. H. Tomlinson invented a recovery boiler [1, 2]. The success of the Kraft process can be attributed to fulfilling the recovery and reuse of inorganic pulping chemicals with the assistance of the recovery boiler. The inorganic chemicals, sodium sulfide (Na_2S) and sodium hydroxide (NaOH), are recovered and recycled during the Kraft process, while the organic matters are burned in recovery boilers to produce steam.

The Kraft process involves four main steps. First, wood chips are cooked at a high temperature and pressure using white liquor (Na_2S plus NaOH). Second, the cooked chips are washed and the spent liquor (weak black liquor) is concentrated in evaporators to produce black liquor. Third, the black liquor is burned in recovery boilers to produce steam and the inorganic component is retained as a molten smelt consisting of Na_2S and sodium carbonate (Na_2CO_3). Lastly, to convert Na_2CO_3 to NaOH, the smelt is dissolved in green liquor and reacted with added lime (CaO), after which the white liquor is recovered, and reused in the cooking process. Subsequently, the amount of lime mud is produced, but the sodium carbonate ($CaCO_3$) in the lime mud can be converted back to the CaO by heating to remove CO_2.

Although the Kraft process shows excellent ability in chemical recycling and energy

requirements, there still exist certain inherent disadvantages that are inevitable, such as poor pulp color, high bleaching costs, and strong odors [3]. Moreover, the stronger pulp fibers produced by the Kraft process when compared to other pulp processes, is typically used to manufacture milk cartons, paper boxes, and brown bags [3].

1.1.2. Black liquor

In the pulp and paper industry, black liquor is a by-product of the cooking process. The dark caramel color of black liquor is due to a large amount of lignin residue. On average, lignin accounts for 35–45% w/w of black liquor solid [4], while the total organic matter only accounts for two-thirds of the solids [5]. Because of the lignin content, the organic matter composition in black liquor range from 10,000 to 120,000 mg $COD \cdot L^{-1}$ [6]. Other primary organic compounds of black liquor include organic acids of low-molecular-weight, hydroxy, and resins [7]. However, the variable organic matter content of black liquor depends primarily on the operational conditions of the pulping process and raw materials. For example, woody biomass black liquor generally has a higher organic-to-inorganic ratio than non-woody counterparts [7].

The black liquor is normally recycled on site through the recovery boiler. In Canadian pulp and paper facilities that use Kraft process, the black liquor should be concentrated to at least 60% solids through evaporators before entering the boiler for adequate combustion [8]. However, a large amount of reduced sulfur compounds can be generated during the Kraft process, especially hydrogen sulfide. The hydrogen sulfide is produced from the reaction between Na_2S in the black liquor and CO_2 in the furnace exhaust [9]. The strong odors in pulp mills are arising from these reduced sulfur compounds which are harmful to

human health.

1.1.3. Lignin

Lignin is one of the three main components of lignocellulosic biomass. The other two main components are cellulose and hemicellulose. Lignin plays a crucial role because lignin serves as the glue to hold the lignocellulose matrix together in plant cell walls. Lignin can also provide plants with high mechanical strength to grow vertically upward and avoid attacks from microorganisms and pathogens. The anti-oxidation characteristics of lignin can protect carbohydrates in plants from being oxidized.

All lignin functions can be associated with the complex structure of lignin, which consists of irregular, random, and three-dimensionally cross-linked polymers of phenylpropane subunits joined by various linkages [10]. Additionally, variability in the lignin structure between different plant species results in the different chemical composition. Typically lignin contains three phenylpropane subunits denoted as p-hydroxyphenyl (H), syringyl (S), and guaiacyl (G), as well as their respective precursors, such as coniferyl, p-coumaroyl, and sinapyl alcohols (Figure 1.1) [11]. However, the fraction of these subunits in lignin varies according to species, tissue type, and cell type, and the structure differs by the number and the position of methoxy groups on the aromatic ring [12].
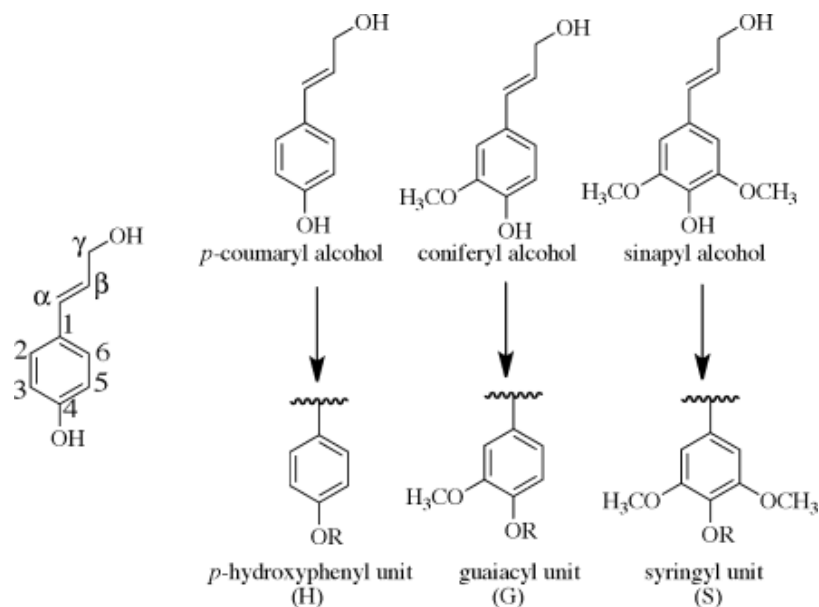
Figure 1.1 Three phenylpropane subunits of lignin and their corresponding precursors [12].

Fewer methoxy groups (H<G<S) leave more vacant reactive sites on rings, leading to more possible linkage options for the polymerization of monolignols. For example, the reactions at number 3 or 5 position on the ring tend to form C—C bonds that are hard to break, while the weaker C—O bond tend to be abundant if most subunits contain one or two methoxy group [12]. β-O-4 alkyl aryl ether linkages (Figure 1.2), as the most abundant linkages derived from C—O bond, account for 45–50% linkages in softwood lignin and 60–62% linkages in hardwood lignin [13].
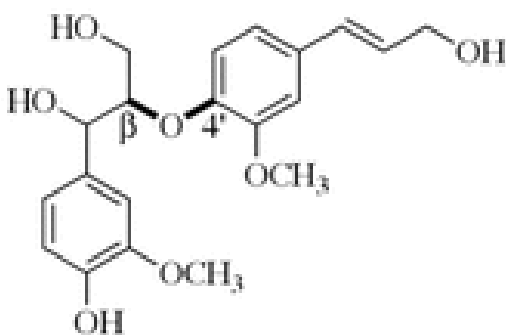
Figure 1.2 β-O-4 alkyl aryl ether linkages [12].

1.1.4. Lignin sources and properties

Several types of lignin are now commercially available in large quantities, such as lignosulfonates, Soda lignin, Kraft lignin, Organosolv lignin, and hydrolyzed lignin. Lignosulfonate is a chemically modified lignin which is derived from the traditional sulfite pulping process [14]. Kraft lignin is produced from cooking soft and hard woods with NaOH and Na_2S. Soda lignin is produced from alkali pulping, and Organosolv lignin is produced by employing organic solvents such as acetone, methanol, ethanol, and acetic acid at relatively high temperatures [15]. Hydrolyzed lignin can be produced from the acid hydrolysis process of straw [16].

1.2. Photocatalysis

1.2.1. Introduction

Photocatalysis refers to the use of photons to drive redox reactions on a photo-illuminated catalyst surface. Photocatalysis can be classified into heterogeneous and homogeneous. In heterogeneous photocatalysis, the photocatalysts are in a different phase than the reactants. The photocatalysts are semiconductors, such as TiO_2 and Zinc oxide (ZnO), but many novel photoactive semiconductors are also proposed, including the oxides of transition metals, such as Nb, and main group elements, such as Ga [17]. Photocatalysis has attracted more attention because of excellent efficiency and low cost [18]. In contrast, in homogeneous photocatalysis, the photocatalysts and the reactants exist in the same phase. For example, the Fenton process is a typical homogeneous photocatalysis, where strong oxidative radical can be produced when Fe (III) is photo-reduced to Fe (II) in the liquid phase [19].

1.2.2. Mechanism of lignin photocatalysis

   The photocatalytic degradation of lignin can be considered as an oxidative degradation which is also classified as an AOP. Lignin can be degraded by several highly reactive radicals, which are generated during semiconductor catalysts being radiated by UV or near-UV light. The UV light excites electrons from the valence band (h_{VB}^+) to the conductive band (e_{CB}^-) to produce a positive hole (Eq. (1.1)) [20]. Next, water (H_2O) or hydroxyl ions (OH^-) reacts and produces hydroxyl radical ($\cdot OH$) in the positive hole (equations 1.2 and 1.3). In this case, the oxidation potential is +2.80 V, a value slightly lower than fluorine, the strongest oxidizing agent [21]. The e_{CB}^- can react with molecular oxygen to produce superoxide anions radical ($\cdot O_2^-$) (Eq. (1.4)) [20]. The $e^- \text{-} h^+$ combination serve as charge carriers which promote redox reactions during the photocatalytic process. However, recombination of the $e^- \text{-} h^+$ causes the disappearance of these charge carriers without any chemical reaction [22] and with the rapid release of heat [23].

$$TiO_2 + h\nu \rightarrow e_{CB}^- + h_{VB}^+ \tag{1.1}$$

$$h_{VB}^+ + H_2O \rightarrow H^+ + \cdot OH \tag{1.2}$$

$$OH^- + h_{VB}^+ \rightarrow \cdot OH \tag{1.3}$$

$$O_2 + e_{CB}^- \rightarrow \cdot O_2^- \tag{1.4}$$
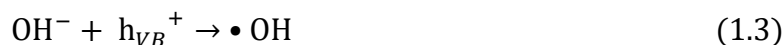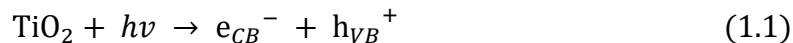
   With regards to the oxidative ability of $\cdot OH$ and $\cdot O_2^-$ for lignin, Gierer [24] suggested that $\cdot OH$ can react with aromatic rings and olefinic groups in the lignin, both of which are electron-rich moieties. Lee [25] reported that $\cdot O_2^-$ could react with phenoxy radicals in lignin structure to form dioxetane. Subsequently, the ring structures can be opened and further oxidized to smaller organic acids. Once the lignin is degraded on the TiO_2 surface,

the intermediates are able to leave the interface region and dissolve into the bulk liquid phase.

1.2.3. The process of photocatalysis

During the UV irradiation, organic compounds undergo a series of steps. First, the organic compounds in the liquid phase diffuse to the TiO_2 surface region. Next, the organic compounds adsorb onto the TiO_2 surface. In the following step, the photon activated TiO_2 initiates the photocatalytic degradation of the adsorbed chemical with a subsequent production of byproducts. Next, the byproducts desorb from the TiO_2 surface and finally, the byproducts leave the interface region and dissolve into the bulk liquid phase [26].

Before full degradation into CO_2 and H_2O is attained, intermediates can be produced by controlling the reaction (Eq. (1.5)) [27]. The determination of CO_2 as well as total organic carbon (TOC) is useful in establishing the efficiency of the reaction [28].

$$\text{Organic compounds} \xrightarrow{TiO_2/h\nu} \text{Intermediate(s)} \longrightarrow CO_2 + H_2O \qquad (1.5)$$

For large molecular weight (MW) chemicals, such as lignin, the MW distribution pattern moves from high MW to low MW during the photocatalytic treatment [29]. This can be explained by the conversion of lignin into short chain carbon compounds [27]. Intermediates from the photocatalysis of lignin and black liquor from literature are summarized in Table 1.1.

Table 1.1 Intermediates examined from lignin and black liquor photocatalysis.

Substrates	Intermediates	Reference
Sodium lignosulfonate	Acetic acid, muconic acid, 2-methylhexadecane	[30]
Lignin precipitate from black liquor	Vanillin, coniferylic alchol, vanillic acid, p-coumanic acid, syringaldehyde	[31]
Kraft lignin	Acetic acid, malonic acid, succinic acid, butylated hydroxytoluene, vanillin, veratric acid, and palmitic acid	[32]
Organosolv black liquor	Syringol, pyrocatechol, vanillin, syringaldehde, sinapyladehyde	[29]
Commercial lignin	Ethylbenzene, acetovanillone, acetosyringone, syringaldehyde, styrene, acetyl vanillin, vanillin, 2,6-dimethoxybenzoquinone, and diisobutyl phthalate	[33]

1.2.4. Semiconductor materials

1.2.4.1. Titanium dioxide (TiO₂)

TiO_2 is generally recognized as the best photocatalyst because of photochemical stability, low cost, and low toxicity [23]. TiO_2 can decompose a variety of organic compounds during UV photocatalysis. UV radiation actuates the photo-excited electrons in TiO_2 with wavelengths below 380 nm [34]. The specific surface area (SSA) and the crystal structure of TiO_2 are two physical characteristics of photocatalysts.

The nanostructures of TiO_2 has been widely used and fabricated with various morphologies and properties. Zero-dimensional TiO_2 is spherical with a high SSA [35]. TiO_2 in one-dimensionality is manufactured into one-dimensional fibers or tubes, whose high surface-to-volume ratio can decrease the recombination rate of e^--h^+ and promote the transfer rate of interfacial charge carriers [36]. TiO_2 in two-dimensionality is normally a two-dimensional nanosheet with high adhesion and smooth surface, and three-dimensional TiO_2 has an interconnecting structure in order to increase the carrier mobility [36].

In nature, TiO_2 exists in the following four crystal forms: anatase, brookite, rutile, and

CHAPTER 1

monoclinic-TiO_2. Among these structural forms, anatase TiO_2 is the best photocatalyst, followed by rutile TiO_2. TiO_2 was first examined by Kobayakawa [37] for lignin photocatalysis. Since then, many studies have investigated TiO_2's catalytic ability to improve photocatalytic degradation of lignin [31, 38].

1.2.4.2. Other semiconductor materials

Using TiO_2 for wastewater treatment is impractical because of the cost. Many researchers have explored the feasibility of other economic alternatives for lignin photocatalysis, such as combining with other components, doping with non-metal atoms, and adding metal ions.

Irie [39] and Yu [40] used TiO_2, grafted with Cu (II) and Fe (III) to enhance the photocatalytic efficiency because highly charge metal ions can accept electrons and subsequently enhance the catalytic process. Yuan [41] loaded activated carbon fibers (ACF) on the TiO_2 to increase the surface area based on the pore structure of ACF; however, the surface area of TiO_2/ACF is moderate in consideration of the synergistic effect between photocatalysis and adsorption. Ma et al. [42] reported an increase in the photocatalytic efficiency of TiO_2 by adding 1.0% w/w Pt. These researchers also reported Pt/TiO_2 performed better under acidic conditions than alkaline conditions. Other new catalysts have been useful and promising. Li et al. [43] proposed to use Ag_{40}-AgCl/ZnO nanorod as a photocatalyst to degrade lignin. They reported the supported catalyst exhibited high photocatalytic activity even under solar light conditions.

1.2.5. Factors affecting photocatalysis

1.2.5.1. The effect of pH

During the irradiation of light, the pH of photocatalyzed lignin solutions will decrease with the irradiation time. This is a result of the enrichment of carboxylic acid groups during the photocatalysis process. For example, Shewa et al. [30] observed a maximum reduction of pH value from 8.0 to 5.9 using 1 $g \cdot L^{-1}$ TiO_2 and 0.5 $g \cdot L^{-1}$ lignosulfonate.

The effect of pH on the photocatalysis is mainly due to the acid-base equilibrium of the hydroxyl group. Additionally, other aspects of explanation include the pH effect on the lignin solubility, linkage stability and various lignin structures [44]. However, the effect of pH on lignin photocatalysis is partially contradictory. For example, Kansal et al. [45] attained the result that the photocatalysis of lignin was favorable at pH = 11. These researchers explained high pH facilitates the formation of •OH. Alternatively, Chang et al. [46] observed a higher reaction rate and a better capacity of lignin decomposition under acidic conditions when compared with alkaline conditions. The maximum lignin degradation efficiency was observed at pH = 3, with 93% at 10 min and 99% at 960 min.

1.2.5.2. The initial concentration of lignin

Lignin photocatalytic degradation also relies on the initial lignin concentration. In general, an initial lignin concentration which can inhibit photodegradation leads to a low decomposition efficiency. Ksibi et al. [31] reported that lowering the initial lignin concentration can enhance the efficiency of lignin photocatalytic degradation. The inhibitory effect of the high initial concentration is mainly due to the lower exposure of the catalyst to the irradiation. This results in inhibiting the production of •OH and $•O_2^-$ which

limits the rate of lignin decomposition.

In contrast, a dilute lignin solution has a less dark color and allows photons to penetrate the solution and subsequently reach the catalyst surface. Kansal [45] and Li [43] observed the same phenomenon using ZnO/TiO$_2$ and Ag-AgCl/ZnO, respectively. Furthermore, Kansal [45] and Li [43] achieved almost 100% lignin removal at a low initial concentration of lignin solution. Li et al. [43] reported that the inhibitory effect becomes more significant when the initial concentration of lignin reaches a threshold value of 50 mg$\cdot$L^{-1}. They also offered a further explanation of this phenomenon that the surface of the photocatalyst is adsorbed with a large number of lignin molecules if the initial concentration is high, resulting in fewer active sites of catalysts.

1.2.5.3. The effect of the photocatalyst dosage

The photocatalyst dosage is also a significant factor affecting photocatalysis. The addition of photocatalysts can enhance the capability to decompose lignin because it can increase the total active surface area; however, an excessive dosage can inhibit the photocatalysis process. For example, Chang et al. [46] reported that for the TiO$_2$/UV system, a removal efficiency of 88% was observed for an optimum level of 10 g$\cdot$L^{-1} TiO$_2$ and a pH = 7. TiO$_2$ levels greater than the optimum level will impair light transmission. This interference causes fewer photons reaching the catalytic surface coupled with reducing the production of e$^-$-h$^+$. Ma et al. [42] reported that the reaction rate constant increased proportionally with the TiO$_2$ dosage until an optimal dosage of 10 g$\cdot$L^{-1}. When the TiO$_2$ dosage exceeded the optimum level, the reaction rate could not be further enhanced. Li et al. [43] achieved almost complete removal of lignin using Ag$_{40}$-AgCl/ZnO

at 4 g·L^{-1}. These researchers also reported that the excessive dosage of catalyst inhibited lignin degradation, and they attributed this phenomenon to the aggregation of catalyst particles at the high concentration. Kansal et al. [45] reported the similar effect of catalyst dosage on lignin degradation, and they achieved the optimum dosage of ZnO at 1 g·L^{-1}.

1.2.5.4. The effect of temperature

Typically, a higher temperature will enhance the photocatalytic reaction rate. Increasing the temperature leads to more free radicals being produced. Moreover, the oxidation rate at the catalyst surface become more faster at higher temperature [47]. Studies by Choquette-Labbé et al. [48] demonstrated that for three temperature conditions at 23°C, 30°C and 37°C, 37°C was optimum condition for phenol photocatalytic degradation. By increasing the temperature from 23°C to 37°C, these researchers reported the phenol degradation rate constant increased by approximately 60% with 5 nm TiO_2. However, increasing temperatures leading to a reduction in the dissolved oxygen level causes the production of fewer radicals [47].

1.2.5.5. The effect of the particle size

TiO_2 particles are typically used within the nanometer range as photocatalysts, whereas the TiO_2 particle size within the micrometer range cannot exhibit an ideal photocatalytic activity [49]. A smaller particle size provides a larger surface area as well as more active sites [50]. Thus, more active sites would be available on the TiO_2 surface, which consequently promotes photocatalytic efficiency. However, as the particle size is reduced to extremely small, the photocatalytic efficiency also decreases. This is attributed to the

quantum size effect [51]. Carneiro et al. [52] investigated the effect of particle size on the photocatalytic activity within the range from 7 nm to 35 nm, and they reported that a threshold level of 15 nm exhibited a minimum activity. Higher or lower than this threshold particle size is more photocatalytically active.

1.2.6. Valuable chemical products of lignin photocatalysis

Lignin, as a polyphenolic chemical, can potentially serve as a sustainable feedstock for producing valuable aromatic compounds. Through the oxidative lignin degradation, some critical linkages within the lignin structure, such as aryl ether bonds, can be selectively broken to produce desired chemicals. Two types of aromatic aldehyde, vanillin, and benzaldehyde can be produced as the main valuable products during the oxidative degradation of model lignin compounds [53].

1.2.6.1. Vanillin

Lignin is used as one of the main raw materials for producing vanillin ($C_8H_8O_3$) [54]. Because of the crucial role of vanillin in the food and cosmetic industries, an increasing number of studies on improving conversion efficiency has been reported in recent years. Raquel et al. [29] found that the optimum exposure time of black liquor to UV radiation for vanillin production is 1h. Wang et al. [55] tested five types of lignin and proposed that vanillin production could be improved significantly by using lignin with a higher content of β-O-4 linkages. However, the yield of vanillin was quite low because of complex lignin structure and a lack of knowledge of the degradation routes. Tarabanko et al. [56] proposed the mechanism of lignin-to-vanillin oxidation conversion and pointed out that the key step

is the cleavage of a bond between the α- and β-carbon atoms of the phenylpropane unit of lignin.

1.2.6.2. Benzaldehyde

Benzyl alcohol, the second most valuable lignin product, is produced from lignin. Because benzyl alcohol is the simplest aromatic alcohol and the photochemical production of benzyl alcohol to benzaldehyde is considered as a lignin model reaction [57]. Higashimoto et al. [58] first revealed that benzyl alcohol can be oxidized by photocatalyst (TiO_2) using visible light. These researchers pointed out that the surface •OH groups on TiO_2 can interact closely with the aromatic structure in benzyl alcohol during the illumination process. Benzyl alcohol has been intensely studied as the model lignin compound to investigate the photocatalytic degradation of lignin. Tanaka et al. [59] proposed that benzyl alcohol can be converted to benzaldehyde in almost equal quantities by the presence of Au/CeO_2 photocatalyst under green light illumination. Additionally, Feng et al. [60] proposed that Ir/TiO_2 prepared by photo-deposition has a remarkable photocatalytic performance on the conversion of benzyl alcohol to benzaldehyde because iridium clusters on the modified TiO_2 surface can suppress the recombination of photo-excited holes and electrons.

1.2.6.3. Biogas

In addition to large MW byproducts, low MW organic byproducts from lignin can be used to produce methane by anaerobic digestion. At the present time, the biogas is normally obtained as end products, instead of a variety of phenolic products, such as vanillin and benzaldehyde. These phenolic compounds with similar characteristics cause

the difficulty in separation and purification, so it is a challenge for mass production of these phenolic product from lignin [61]. Due to the recalcitrance nature of lignin, anaerobic digestion of lignin needs to be carried out via a pretreatment step. Various pretreatment methods have been studied for improving the production of biogas. Li et al. [43] reported that biogas yields from degraded lignin samples after photocatalytic treatment by Ag_{40}-AgCl/ZnO increased by 23.1% in comparison to untreated lignin samples.

1.3. Current optimization methods

1.3.1. One-factor-at-a-time (OFAT)

OFAT is a monothetic optimization method. One factor is selected to test every time, and other factors are kept constant to find the optimum amount of the factor of interest. Many researchers have used this conventional method to optimize several parameters in lignin photocatalysis at the early stage. For example, Chang et al. [46] designed their experiments using OFAT to optimize pH level and TiO_2 dosage. Kansal et al. [45] optimized the lignin percentage degradation by changing the ZnO dose, pH, oxidant concentration, and lignin concentration. Li et al. [43] also designed their experiments based on OFAT to optimize the experimental parameters for the new photocatalyst, Ag_{40}-AgCl/ZnO nanorods, including initial pH value, catalyst dosage, initial lignin concentration, and holes/radicals scavengers.

Although OFAT has been used to optimize the process of lignin photocatalytic degradation, experimental design based on OFAT cannot be used to test several parameters simultaneously. In general, the OFAT results in numerous time-consuming and costly experimental designs. Moreover, the interaction between several variables cannot be

identified by employing OFAT. Experimental analysis based on OFAT will lead to the misinterpretation of results and less predictive ability for varying operating conditions. When compared to OFAT, statistical modeling tools and multi-variable design of experiment (DOE) are preferred for the optimizing experimental design.

1.3.2. The 2^k factorial design

2^k factorial design is used to consider an experiment that involves k factors. Each factor is designed at only two levels, the "high" and "low" level. For a three-factor 2^k design, the factor points are located at every corner of a cube (Figure 1.3). As is similar with other factorial designs, the 2^k factorial design is a method which will lead to developing a statistical model that depicts the main factor effects and factor interaction effects. The model is characterized by investigating all the factors with a minimal number of experiments. This feature of the 2^k factorial design is used usually in the early stages of experimental work. In the case of two levels, the response is assumed linear over the range of factors [62].
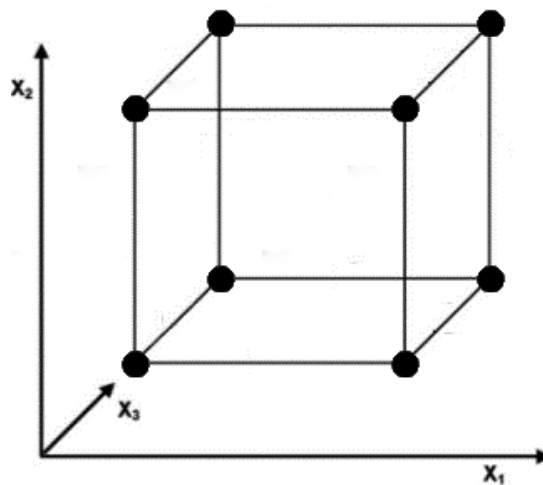
Figure 1.3 Graphical representation of a 2^3-factorial design.

The 2^k factorial design can also be applied to optimize photocatalysis. Shoko et al. [63] reported experiments on the basis of a 2^3-factorial design, where sodium lignosulfonate (LS) concentration, TiO_2 concentration and pH were examined. A second-order regression model was developed in their study, involving the second-order intersections between each factor and the main effect of each factor. Through the interaction effect analysis, they reported that at the low-pH region, decreasing catalyst concentration and increasing substrate concentration can optimize the reaction rate, while at the high-pH region, increasing catalyst concentration and decreasing substrate concentration can optimize the reaction rate [63].

1.3.3. Box-Behnken design (BBD)

To minimize the number of experiments and obtain an acceptable precision level, the BBD is a suitable design method. The BBD is a rotatable or near rotatable second-order designs based on three-level incomplete factorial designs. In terms of three-factors BBD design, the distribution of parameter points is graphically represented in Figure 1.4, where the parameter points are located at the center and middle edges of a cube [64].
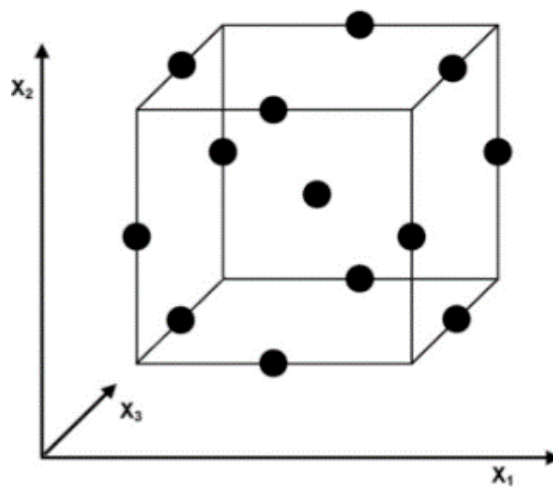
Figure 1.4 Graphical representation of BBD [64].

The experiments designed by using BBD can be optimized using RSM. The RSM method can be summarized as a second-order model (Eq. (1.6)) [30]:

$$y = \beta_0 + \sum_{i=1}^{k} \beta_i x_i + \sum_{i=1}^{k} \beta_{ii} x_i^2 + \sum \sum_{i<j=2}^{k} \beta_{ij} x_i x_j + \varepsilon \qquad (1.6)$$

where β_0 is a constant, β_i is the linear coefficient, β_{ii} is the squared coefficient, β_{ij} is the cross-product coefficient, y is the response variable, x_i and x_j are independent variables, and ε is the "error" in the system.

The BBD technique has been employed to optimize the photocatalysis process. Ray et al. [51] designed four parameters of phenol photocatalysis using BBD with the following factors: TiO_2 concentration, TiO_2 size, dissolved phenol concentration, and oxygen concentration. These researchers developed a quadratic model based on the RSM. The model predicted a maximum degradation rate (0.083 min^{-1}) with the optimum conditions set at 1.0 $g \cdot L^{-1}$ TiO_2, 9.09 nm TiO_2 particle size, 40 $mg \cdot L^{-1}$ phenol, and 31 $mg \cdot L^{-1}$ dissolved oxygen concentration. Shewa et al. [65] selected three parameters of a model lignin compound based on the following BBD factors: TiO_2 concentration, substrate concentration, and revolutions per minute (RPM). These researchers reported developing a quadratic model where the response variable was the BOD_5 to COD ratio. This model predicted a maximum $[BOD_5]/[COD]$ ratio (0.386) with the ideal condition set at 944 $mg \cdot L^{-1}$ TiO_2 concentration, 569 mg $COD \cdot L^{-1}$ substrate concentration, and 9 RPM for the mixing rate. In comparison, the optimum conditions by OFAT was 1 $g \cdot L^{-1}$ TiO_2 concentration, 683 mg $COD \cdot L^{-1}$ substrate concentration, and 10 RPM for the mixing rate [30].

1.4. Summary of research objectives

The present study aimed to optimize the black liquor photocatalytic degradation. TiO_2 was used as a photocatalyst with UV light as the light source and TOC was selected as the response variable. Five factors investigated as variables for the optimization study included black liquor concentration, TiO_2 concentration, initial pH, operation temperature and TiO_2 particle size. These variables were optimized in two groups.

The first group is discussed in Chapter 3 and included the black liquor concentration and TiO_2 concentration. The two objectives for Chapter 3 are as follows:

1) Evaluate the importance of black liquor concentration and TiO_2 concentration on the TOC removal efficiency, and

2) Determine the optimal composition of black liquor concentration and TiO_2 concentration as the preliminary optimization.

Chapter 4 offers an overview of the second group of factors that were studied as the primary factors. These include initial pH, operation temperature, and TiO_2 particle size. The objectives of this study are as follows:

1) Evaluate the effect of the initial pH, temperature, and TiO_2 particle size on the degradation of black liquor based on TOC removal,

2) Develop a predictive model involving these three common factors for black liquor degradation based on the TOC removal, and

3) Maximize the TOC removal efficiency by identifying the initial pH, temperature, and catalyst particle size.

1.5. References

[1] C.J. Biermann, Pulping fundamentals, in: C.J. Biermann (Ed.), Handbook of pulping and papermaking, Academic Press, San Diego, 1996, pp. 55–100.

[2] C.J. Biermann, Kraft spent liquor recovery, in: C.J. Biermann (Ed.), Handbook of pulping and papermaking, Academic Press, San Diego, 1996, pp. 101–122.

[3] P.J. Chenier, PuIp, paper, and wood, in: P.J. Chenier (Ed.), Survey of industrial chemistry, Springer Verlag Inc., New York, 2002, pp. 399–416.

[4] S. Chaudhry, R. Paliwal, Techniques for remediation of paper and pulp mill effluents: Processes and constraints, in: C.M. Hussain (Ed.), Handbook of environmental materials management, Springer International Publishing, New York, 2018, pp. 1–19.

[5] H. Niemi, J. Lahti, H. Hatakka, S. Karki, S. Rovio, M. Kallioinen, M. Manttari, M. Louhi-Kultanen, Fractionation of organic and inorganic compounds from black liquor by combining membrane separation and crystallization, Chem. Eng. Technol. 34 (2011) 593–598.

[6] G. Huang, J.X. Shi, T.A.G. Langrish, A new pulping process for wheat straw to reduce problems with the discharge of black liquor, Bioresour. Technol. 98 (2007) 2829–2835.

[7] P. Bajpai, Properties, composition, and analysis of black liquor, in: P. Bajpai (Ed.), Pulp and paper industry, Elsevier Science, New York, 2016, pp. 25–36.

[8] C. Ballard, Technical standards to manage air pollution, Ministry of the Environment and Climate Change, Toronto, 2018.

[9] N.P. Cheremisinoff, P.E. Rosenfeld, Sources of air emissions from pulp and paper mills, in: N.P. Cheremisinoff, P.E. Rosenfeld (Eds.), Handbook of pollution prevention and cleaner production, William Andrew Publishing, Oxford, 2010, pp. 179–259.

[10] R. Chandra, Environmental waste management, CRC Press, Boca Raton, 2015.

[11] F. Hu, A. Ragauskas, Pretreatment and lignocellulosic chemistry, Bioenerg. Res. 5 (2012) 1043–1066.

[12] A.K. Sangha, L. Petridis, J.C. Smith, A. Ziebell, J.M. Parks, Molecular simulation as a tool for studying lignin, Environ. Prog. Sustain. Energ. 31 (2012) 47–54.

[13] S. Guadix-Montero, M. Sankar, Review on catalytic cleavage of C–C inter-unit linkages in lignin model compounds: Towards lignin depolymerisation, Top. Catal. 61 (2018) 183–198.

[14] W.G. Glasser, Lignin-based polymers, in: K.H.J. Buschow (Ed.), Encyclopedia of materials: Science and technology, Elsevier, Oxford, 2001, pp. 1–7.

[15] K. Merklein, S.S. Fong, Y. Deng, Biomass utilization, in: C.A. Eckert, C.T. Trinh (Eds.), Biotechnology for biofuel production and optimization, Elsevier, Amsterdam, 2016, pp. 291–324.

[16] P. Chen, Q. Zhang, R. Shu, Y. Xu, L. Ma, T. Wang, Catalytic depolymerization of the hydrolyzed lignin over mesoporous catalysts, Bioresour. Technol. 226 (2017) 125–131.

[17] M.D. Hernández-Alonso, F. Fresno, S. Suárez, J.M. Coronado, Development of alternative photocatalysts to TiO_2: Challenges and opportunities, Energ. Environ. Sci. 2 (2009) 1231–1257.

[18] R. Saravanan, F. Gracia, A. Stephen, Basic principles, mechanism, and challenges of photocatalysis, in: M.M. Khan, D. Pradhan, Y. Sohn (Eds.), Nanocomposites for visible light-induced photocatalysis, Springer International Publishing, New York, 2017, pp. 19–40.

[19] V. Kitsiou, N. Filippidis, D. Mantzavinos, I. Poulios, Heterogeneous and homogeneous photocatalytic degradation of the insecticide imidacloprid in aqueous solutions, Appl. Catal. B-Environ. 86 (2009) 27–35.

[20] M. Boroski, A.C. Rodrigues, J.C. Garcia, L.C. Sampaio, J. Nozaki, N. Hioka, Combined electrocoagulation and TiO_2 photoassisted treatment applied to wastewater effluents from pharmaceutical and cosmetic industries, J. Hazard. Mater. 162 (2009) 448–454.

[21] M. Umar, H.A. Aziz, Photocatalytic degradation of organic pollutants in water, in: M.N. Rashed (Ed.), Organic pollutants–monitoring, risk and treatment, Intech, London, 2012, pp. 195-209.

[22] B. Ohtani, Titania photocatalysis beyond recombination: A critical review, Catalysts 3 (2013) 942–953.

[23] J. Schneider, M. Matsuoka, M. Takeuchi, J. Zhang, Y. Horiuchi, M. Anpo, D.W. Bahnemann, Understanding TiO_2 photocatalysis: Mechanisms and materials, Chem. Rev. 114 (2014) 9919–9986.

[24] J. Gierer, Formation and involvement of superoxide (O_2^-/$HO_2\cdot$) and hydroxyl ($OH\cdot$) radicals in TCF bleaching processes: A review, Holzforschung 51 (1997) 34–46.

[25] O. Lee, Mechanistic studies of the oxidation of lignin and cellulose models, in: B.J.W Cole, R.C. Fort (Eds.), Ph.D. Thesis, University of Maine, 2003.

[26] H. Dong, G. Zeng, L. Tang, C. Fan, C. Zhang, X. He, Y. He, An overview on limitations of TiO_2-based particles for photocatalytic degradation of organic pollutants and the corresponding countermeasures, Water Res. 79 (2015) 128–146.

[27] J.A. Lalman, W.A. Shewa, Microbial fuel cell for generating electricity, and process for producing feedstock chemicals, US20160064758A1, 2016.

[28] L. Jingfei, S. Yue, L. Yanyan, P. Yaron, The structural, photocatalytic property characterization and enhanced photocatalytic activities of novel photocatalysts Bi_2GaSbO_7 and Bi_2InSbO_7 during visible light irradiation, Materials 9 (2016) 801.

[29] R. Prado, X. Erdocia, J. Labidi, Effect of the photocatalytic activity of TiO_2 on lignin depolymerization, Chemosphere 91 (2013) 1355–1361.

[30] W.A. Shewa, Converting low value lignocellulosic residues into valuable products using photo and bioelectrochemical catalysis, in: J. Lalman (Ed.), Ph.D. Thesis, University of Windsor, 2016.

[31] M. Ksibi, S.B. Amor, S. Cherif, E. Elaloui, A. Houas, M. Elaloui, Photodegradation of lignin from black liquor using a UV/TiO_2 system, J. Photoch. Photobio. A Chem. 154 (2003) 211–218.

[32] K. Kamwilaisak, P.C. Wright, Investigating laccase and titanium dioxide for lignin degradation, Energ. Fuel. 26 (2012) 2400–2406.

[33] V. Nair, P. Dhar, R. Vinu, Production of phenolics via photocatalysis of ball milled lignin–TiO_2 mixtures in aqueous suspension, RSC Adv. 6 (2016) 18204–18216.

[34] R.W. Matthews, Photocatalytic oxidation of organic contaminants in water: An aid to environmental preservation, Pure. Appl. Chem. 64 (1992) 1285–1290.

[35] B. Liu, K. Nakata, M. Sakai, H. Saito, T. Ochiai, T. Murakami, K. Takagi, A. Fujishima, Mesoporous TiO_2 core–shell spheres composed of nanocrystals with exposed high-energy facets: Facile synthesis and formation mechanism, Langmuir 27 (2011) 8500–8508.

[36] K. Nakata, A. Fujishima, TiO$_2$ photocatalysis: Design and applications, J. Photochem. Photobiol. C Photochem. Rev. 13 (2012) 169–189.

[37] K. Koichi, S. Yuichi, N. Shigeo, F. Akira, Photodecomposition of kraft lignin catalyzed by titanium dioxide, Bull. Chem. Soc. Jpn. 62 (1989) 3433–3436.

[38] K. Tanaka, R.C.R. Calanag, T. Hisanaga, Photocatalyzed degradation of lignin on TiO$_2$, J. Mol. Catal. A Chem. 138 (1999) 287–294.

[39] H. Irie, K. Kamiya, T. Shibanuma, S. Miura, D.A. Tryk, T. Yokoyama, K. Hashimoto, Visible light-sensitive Cu(II)-grafted TiO$_2$ photocatalysts: Activities and X-ray absorption fine structure analyses, J. Phys. Chem. C 113 (2009) 10761–10766.

[40] H. Yu, H. Irie, Y. Shimodaira, Y. Hosogi, Y. Kuroda, M. Miyauchi, K. Hashimoto, An efficient visible-light-sensitive Fe(III)-grafted TiO$_2$ photocatalyst, J. Phys. Chem. C 114 (2010) 16481–16487.

[41] R. Yuan, R. Guan, P. Liu, J. Zheng, Photocatalytic treatment of wastewater from paper mill by TiO$_2$ loaded on activated carbon fibers, Colloids. Surf. A Physicochem. Eng. Asp. 293 (2007) 80–86.

[42] Y.S. Ma, C.N. Chang, Y.P. Chiang, H.F. Sung, A.C. Chao, Photocatalytic degradation of lignin using Pt/TiO$_2$ as the catalyst, Chemosphere 71 (2008) 998–1004.

[43] H. Li, Z. Lei, C. Liu, Z. Zhang, B. Lu, Photocatalytic degradation of lignin on synthesized Ag–AgCl/ZnO nanorods under solar light and preliminary trials for methane fermentation, Bioresour. Technol. 175 (2015) 494–501.

[44] C.A. Lekelefac, N. Busse, M. Herrenbauer, P. Czermak, Review article photocatalytic based degradation processes of lignin derivatives, Int. J. Photoenerg. 2014 (2015) 1–18.

[45] S.K. Kansal, M. Singh, D. Sud, Studies on TiO_2/ZnO photocatalysed degradation of lignin, J. Hazard. Mater. 153 (2008) 412–417.

[46] C.N. Chang, Y.S. Ma, G.C. Fang, A.C. Chao, M.C. Tsai, H.F. Sung, Decolorizing of lignin wastewater using the photochemical UV/TiO_2 process, Chemosphere 56 (2004) 1011–1017.

[47] H. Zangeneh, A.A.L. Zinatizadeh, M. Habibi, M. AkiaM, H. Isa, Photocatalytic oxidation of organic dyes and pollutants in wastewater using different modified titanium dioxides: A comparative review, J. Ind. Eng. Chem. 26 (2015) 1–36.

[48] M. Choquette-Labbe, W.A. Shewa, J.A. Lalman, S.R. Shanmugam, Photocatalytic degradation of phenol and phenol derivatives using a nano-TiO_2 catalyst: Integrating quantitative and qualitative factors using response surface methodology, Water 6 (2014) 1785–1806.

[49] T.L. Hathway, Titanium dioxide particle size effects on the degradation of organic molecules, in: W. Jenks, R. Larock, H. Stauffer (Eds.), Thesis, Lowa State University, 2007.

[50] Z. Zhang, C.C. Wang, R. Zakaria, J.Y. Ying, Role of particle size in nanocrystalline TiO_2-based photocatalyst, J. Phys. Chem. B 102 (1998) 10871–10878.

[51] S. Ray, J.A. Lalman, N. Biswas, Using the Box-Benkhen technique to statistically model phenol photocatalytic degradation by titanium dioxide nanoparticles, Chem. Eng. J. 150 (2009) 15–24.

[52] J.T. Carneiro, T.J. Savenije, J.A. Moulijn, G. Mul, Toward a physically sound structure–activity relationship of TiO_2-based photocatalysts, J. Phys. Chem. C 114 (2010) 327–332.

[53] S.H. Li, S. Liu, J.C. Colmenares, Y.J. Xu, A sustainable approach for lignin valorization by heterogeneous photocatalysis, Green Chem. 18 (2016) 594–607.

[54] N. Wongtanyawat, P. Lusanandana, N. Khwanjaisakun, P. Kongpanna, J. Phromprasit, L. Simasatitkul, S. Amornraksa, S. Assabumrungrat, Comparison of different kraft lignin-based vanillin production processes, Comput. Chem. Eng. 117 (2018) 159–170.

[55] Y. Wang, S. Sun, F. Li, X. Cao, R. Sun, Production of vanillin from lignin: The relationship between β-O-4 linkages and vanillin yield, Ind. Crops Prod. 116 (2018) 116–121.

[56] V.E. Tarabanko, D.V. Petukhov, G.E. Selyutin, New mechanism for the catalytic oxidation of lignin to vanillin, Kinet. Catal. 45 (2004) 569–577.

[57] J.C. Colmenares, R. Luque, Heterogeneous photocatalytic nanomaterials: Prospects and challenges in selective transformations of biomass-derived compounds, Chem. Soc. Rev. 43 (2014) 765–778.

[58] S. Higashimoto, N. Kitao, N. Yoshida, T. Sakura, M. Azuma, H. Ohue, Y. Sakata, Selective photocatalytic oxidation of benzyl alcohol and its derivatives into corresponding aldehydes by molecular oxygen on titanium dioxide under visible light irradiation, J. Catal. 266 (2009) 279–285.

[59] A. Tanaka, K. Hashimoto, H. Kominami, Preparation of Au/CeO$_2$ exhibiting strong surface plasmon resonance effective for selective or chemoselective oxidation of alcohols to aldehydes or ketones in aqueous suspensions under irradiation by green light, J. Am. Chem. Soc. 134 (2012) 14526–14533.

[60] W. Feng, G. Wu, L. Li, N. Guan, Solvent-free selective photocatalytic oxidation of benzyl alcohol over modified TiO$_2$, Green Chem. 13 (2011) 3265–3272.

[61] W. Den, V.K. Sharma, M. Lee, G. Nadadur, R.S. Varma, Lignocellulosic biomass transformations via greener oxidative pretreatment processes: Access to energy and value-added chemicals, Front. Chem. 6 (2018) 141.

[62] D.C. Montgomery, The 2^k factorial design, in: D.C. Montgomery (Ed.), Design and analysis of experiments, John Wiley and Sons, Inc., Hoboken, 2012, pp. 752.

[63] E. Shoko, J.C.D. Costa, E.T. White, Optimization of the reaction rate in the photocatalytic degradation of sodium lignosulfonate in a TiO_2 slurry reactor: A multivariate study with response surface analysis, Dev. Chem. Eng. Min. Process. 12 (2004) 475–489.

[64] S.L.C. Ferreira, R.E. Bruns, H.S. Ferreira, G.D. Matos, J.M. David, G.C. Brandão, E.G.P. Silva, L.A. Portugal, P.S. Reis, A.S. Souza, W.N.L. Santos, Box-Behnken design: An alternative for the optimization of analytical methods, Anal. Chim. Acta 597 (2007) 179–186.

[65] W.A. Shewa, J.A. Lalman, S.R. Chaganti, D.D. Heath, Electricity production from lignin photocatalytic degradation byproducts, Energ. 111 (2016) 774–784.

CHAPTER 2

MATERIALS AND EXPERIMENTAL METHODS

2.1. Introduction

In this chapter, the chemicals and instruments used in the experiments and chemical analysis are discussed in the following sections:

a) Chemicals

b) Characterization of experimental and analytical instruments

Note: The chemicals, experimental and analytical instruments, and detailed experimental process in this chapter will be referenced in subsequent chapters.

2.2. Chemicals

The black liquor was obtained from a pulp and paper mill located in Lakehead, Ontario, Canada. Five nm and 15 nm TiO_2 nanoparticles were purchased from Alfa Aesar (Ward Hill, Massachusetts), and 25 nm TiO_2 nanoparticles were purchased from (Evonik Industries, Essen). HCl (37% w/w), H_3PO_4 (85% w/w), and NaOH (97% purity) were purchased from Fisher Scientific (Ontario, Canada).

2.3. Characterizations of experimental and analytical instruments

2.3.1. Photocatalytic reactor

The photocatalytic experiments were conducted using 25 mm ID × 250 mm length quartz tubes (Technical Glass Products Inc., Painesville). The quartz tubes were positioned in a modified Rayonet RPR-100 UV photocatalytic chamber (Southern New England Ultraviolet Co., Branford), as displayed in Figure 2.1 [1].
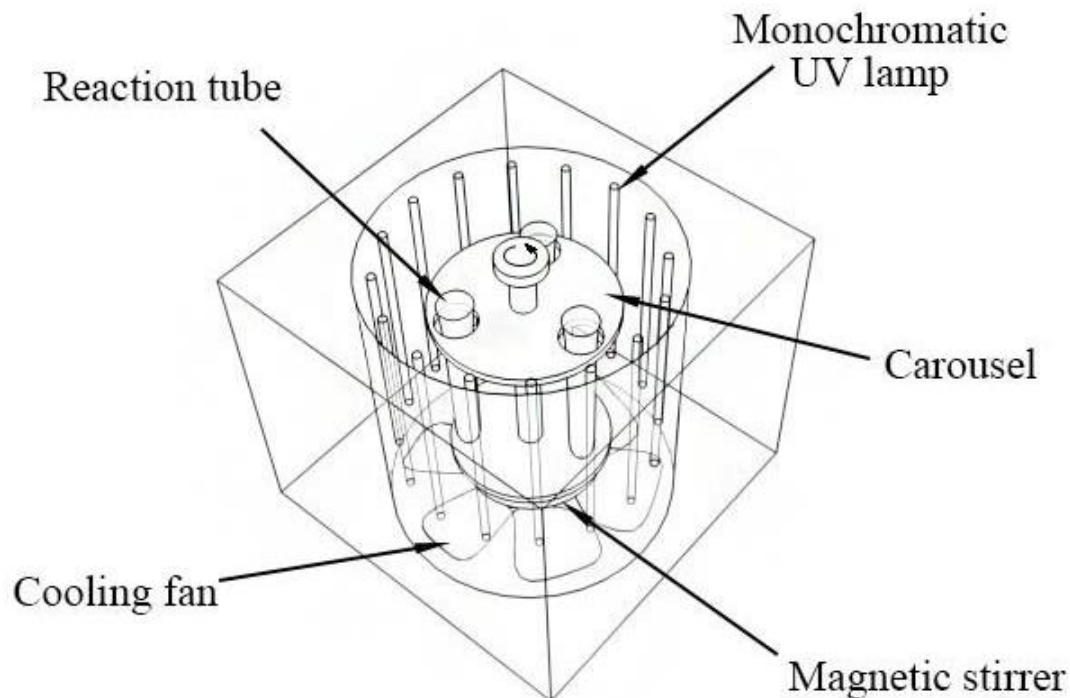
Figure 2.1 Photoreactor schematic.

This chamber was installed with sixteen monochromatic UV lamps (Southern New England Ultraviolet Co., Branford) on the outer perimeter of the photoreactor and a centrally located rotary inner carousel. To minimize the error of UV irradiance between each reaction tube, the carousel was rotated at a fixed rotating speed [2]. The UV lamps are able to emit 300 nm UV light with an average intensity of 9 mW·cm^{-2}. The intensity was measured using a UV-X radiometer equipped with a 300 nm UV sensor (UV Process Supply, Chicago).

The reactor tubes are placed on the rotary carousel and the reaction mixture were magnetically stirred. Stirring ensure the catalyst (TiO$_2$ particle) remain in suspension and also prevent particle agglomeration. The temperature of the photoreactor in this study was performed at 37±2 °C. One hour before initiating the experiment, the photoreactor and UV lamps were turned on to warm up the UV lamps and obtain a stable light density during

the photocatalytic experiment [3]. The mixture volume contained in each tube was 50 mL, and the solutions were prepared by 40 mL Milli-Q® water, 5 mL TiO_2 mixture and 5 mL catalyst solution.

2.3.2. Total organic carbon (TOC) instrument

The TOC analysis was conducted using a TOC-L (Shimadzu, Kyoto) instrument. TOC-L is an instrument that has been used to analyze inorganic carbon (IC), total carbon (TC), and TOC content. TC can be measured through the carbon dioxide generated from the combustion of a sample under 680 ℃ with a platinum catalyst. Likewise, IC can be measured through the carbon dioxide generated from acidification and sparging under pH < 3 of a sample. In addition, TOC can be determined by subtracting the IC concentration from the TC concentration [4].

2.4. References

[1] M. Choquette-Labbe, W.A. Shewa, J.A. Lalman, S.R. Shanmugam, Photocatalytic degradation of phenol and phenol derivatives using a nano-TiO_2 catalyst: Integrating quantitative and qualitative factors using response surface methodology, Water (2014) 1785–1806.

[2] S. Ray, J.A. Lalman, N. Biswas, Using the Box-Benkhen technique to statistically model phenol photocatalytic degradation by titanium dioxide nanoparticles, Chem. Eng. J. 150 (2009) 15–24.

[3] W.A. Shewa, Converting low value lignocellulosic residues into valuable products using photo and bioelectrochemical catalysis, in: J. Lalman (Ed.), Ph.D. Thesis, University of Windsor, 2016.

[4] SHIMADZU, TOC-L laboratory total organic carbon analyzers, https://www.ssi.shimadzu.com/products/toc-analyzers/toc-l-combustion-catalytic-oxidation-method.html (accessed July 15, 2019).

CHAPTER 3

OPTIMAL CONDITIONS FOR BLACK LIQUOR PHOTOCATALYSIS

3.1. Introduction

Black liquor, a major stream which is produced during Kraft pulp and paper mills, is characterized with a highly concentrated organic content. Toxic chemicals in black liquor includes fatty acids, resin acids, and chlorinated phenols [1]. The type of chemicals and concentration are important factors when considering utilizing a biological process for treating wastewaters or upgrading a waste stream into fuels and chemicals. In this study, a photochemical method was considered as an alternative to a biological process.

Photocatalytic oxidation is considered as an approach for black liquor degradation. This approach has great potential to degrade or depolymerize organic compounds [2, 3]. Black liquor from the Kraft mill process can be photodegraded utilizing catalysts such as ZnO and TiO_2 [4]. The photocatalysis process is dependent on factors such as catalyst concentration, substrate concentration, pH and temperature. Optimizing these conditions can be accomplished by employing RSM. RSM is a statistical process which can be employed to model and analyze a process in which the response variable is impacted by several factors.

The 2^k factorial study can be used to determine low and high limits of different factors that affect the response variable, and to determine optimum conditions. This study revealed the appropriate black liquor and TiO_2 concentrations. These concentrations were employed to conduct the BBD study.

As discussed in the literature review, the substrates concentration and the catalyst

concentration could affect the photocatalysis. The dilute black liquor solution has a less dark color which will allow more photons to reach the catalyst surface. Shewa and Lalman [5] used 500 mg·L^{-1} lignosulfonate, a model lignin chemical, to investigate the effects of several parameters on the photocatalysis process. Preliminary experimental work indicated high black liquor concentration such as 920 mg TS·L^{-1} was inhibitory towards light transmission to the catalyst surface. A black liquor concentration under 460 mg TS·L^{-1} was selected for conducting further studies.

The catalyst concentration can also impact light transmission and hence, photocatalysis. Shewa and Lalman [5] examined the impact of the catalyst loading on the degradation of lignosulfonate by changing the concentration of TiO$_2$ between 0.5 g·L^{-1} and 3.5 g·L^{-1}, and the highest COD reduction was observed when employing 1 g·L^{-1} catalyst. In similar studies, Ray et al. [6] using 1 g·L^{-1} catalyst to examine the photocatalytic degradation of phenol.

The photocatalytic reaction time will also affect the quantity of black liquor degraded. With an irradiation time from 1 to 6 hours, Lalman and Shewa [7] reported a maximum production of biodegradable intermediates from lignin photocatalysis was achieved at 4±0.5 hours. Hence, in this study, all photocatalytic experiments were conducting using a 4-hour UV irradiation time.

3.2. Materials and methods

3.2.1. Chemicals

Black liquor was obtained from a pulp and paper mill located in Lakehead, Ontario, Canada. After weighing the TiO$_2$ and adding it to Milli-Q® water, the stock suspensions

of TiO$_2$ nanoparticles were prepared and stored at 23 ± 2 °C in 100 mL serum bottles. The TiO$_2$ stock solution was sonicated using an ultrasonic bath procured from VWR (Mississauga, Ontario) for 15 to 20 minutes. This process produced a homogeneous suspension which was used to deliver a more accurate quantity of catalyst to the diluted black liquor solution.

3.2.2. Statistical design: 2^k factorial design

A 2^k factorial design is mainly used for preliminary study of the factors' effect on the response variable and for determining the optimum condition. Two levels of every factor, the "high" and "low", are used to provide the smallest number of experimental runs to study k factors in a complete factorial design [8].

In this study, the 2^k factorial design is used as the experiment design basis. Two factors, black liquor concentration, and TiO$_2$ concentration, are denoted by A and B and evaluated at a high and low level. Thus, this is designated as a two-square factorial design and the experiments under four combinations of conditions were carried out (Table 3.1).

Table 3.1 Two square factorial design of black liquor and TiO$_2$ concentration.

Exp. #	Factor combination		Black liquor concentration (mg TS·L^{-1})	TiO$_2$ concentration (g·L^{-1})
	A	B		
1	Low	Low	230	1
2	High	Low	460	1
3	Low	High	230	2
4	High	High	460	2
5	Low	Low	230	1
6	High	Low	460	1
7	Low	High	230	2
8	High	High	460	2

In consideration of the cost of chemicals, the study based on factorial design is normally conducted with one replicate or known as an un-replicated factorial design [8]. However, in the case of only two factors involved in this study, the experiments were performed with two replicates for accuracy. Minitab (Minitab Inc., State College, PA) was used to determine the impacts of each factor on the response. This software can also examine the significance of their interaction effects on the response variable. The percent TOC removed was selected as the response. Finally, the ANOVA verified the significance of every term of the RSM model. The experiments were performed in duplicate.

3.2.3. Sampling and analytical methods

3.2.3.1. Sample collected

Five mL samples were collected from the reaction tubes at 30-minute intervals and subsequently centrifuged (Sorvall ST 16 Thermo Scientific, Ontario, Canada) at 4500 RPM for 25 to 35 min to separate the TiO_2 catalyst from the diluted black liquor. Subsequently, the black liquor samples were stored in sealed vials for TOC determination.

3.2.3.2. TOC analysis

The TOC analysis was analyzed using a TOC-L instrument (Shimadzu, Kyoto). HCl (37% w/w) and H_3PO_4 (85% w/w) were purchased from Fisher Scientific (Ontario, Canada). The black liquor samples were diluted 3-fold before analysis.

3.2.4. Other instruments and materials

The black liquor and catalyst mixture were stirred under dark conditions for 45 minutes

in an oven set a desired temperature before photocatalysis. This pretreatment step ensured

the reaction mixture was thoroughly mixed.

3.3. Results and discussion

3.3.1. Statistical summary and analysis

The percent TOC removed during the degradation of black liquor over a 4 h period was

used as the response variable (Table 3.2).

Table 3.2 Percentage TOC removal.

Condition #	Factors		% TOC removed	
	Black liquor concentration (mg TS·L^{-1})	TiO$_2$ concentration (g·L^{-1})	Sample #1	Sample #2
1	230	1	25.3	24.6
2	460	1	13.8	16.8
3	230	2	34.2	38.2
4	460	2	19.3	15.2

Note: The TOC measurement includes residual black liquor organics plus the degradation by-products.
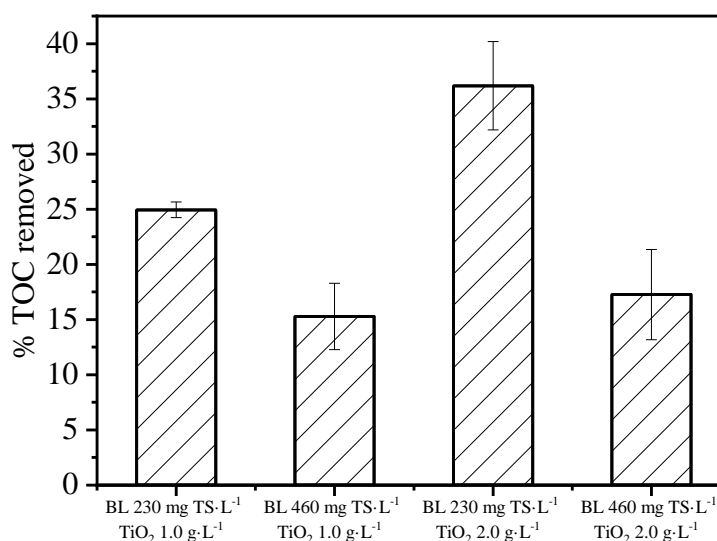

Figure 3.1 Percent TOC removed for four conditions.
Note: BL = Black liquor, and the TOC measurement includes residual black liquor organics plus the degradation by-products.

Among the four conditions shown in Figure 3.1, the greatest TOC removal was observed at $36.2 \pm 4.0\%$ for 230 mg $TS \cdot L^{-1}$ black liquor and 2 $g \cdot L^{-1}$ TiO_2. In contrast, the lowest TOC removal was observed at $15.3 \pm 3.0\%$ for 460 mg $TS \cdot L^{-1}$ black liquor and 1 $g \cdot L^{-1}$ TiO_2. Note, the percent TOC removed was approximately doubled going from the minimum removal value to the maximum. Estimating the impact of every single factor on the percent TOC removed is a crucial component for conducting the BBD. Increasing the TiO_2 concentration caused an increase in the percent TOC removed when comparing conditions 1 and 3. In comparison, a slight increase in the percent TOC removed was observed when comparing conditions 2 and 4. The increase in the percent TOC removed is because 230 mg $TS \cdot L^{-1}$ black liquor allows more photons to penetrate the solution and subsequently to reach the TiO_2 surface than 460 mg $TS \cdot L^{-1}$ black liquor, and 2 $g \cdot L^{-1}$ TiO_2 provides more catalyst active sites than 1 $g \cdot L^{-1}$ TiO_2. A normal probability plot confirmed the individual and interaction effects on the response variable (Figure 3.2).

3.3.2. Preliminary effect analysis

The normal probability plot of two experimental factors is shown in Figure 3.2. Points close or on the straight line indicate negligible effect on the response, while points showing large effects are situated away from the line. As shown in Figure 3.2, all the three points (A = black liquor concentration, B = TiO_2 concentration, and AB = interaction between A and B) are located away from the straight line and hence, they have a significant effect on the percent TOC removed [9].
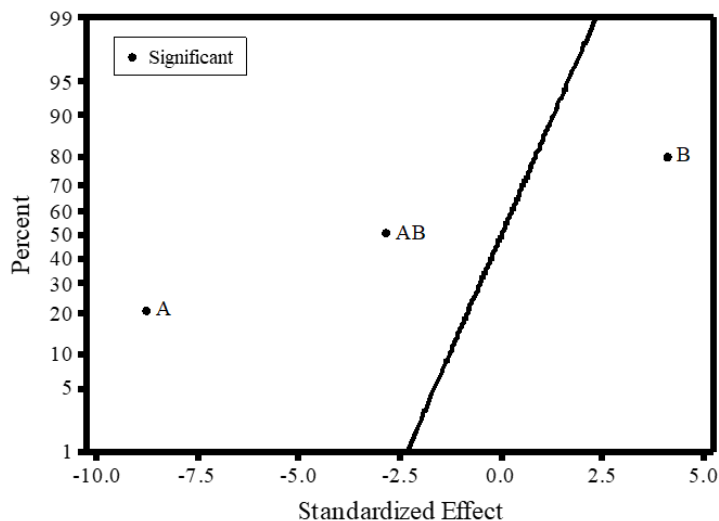
Figure 3.2 Normal probability plot of two experimental factors.
Note: A = black liquor concentration, B = TiO$_2$ concentration, AB = interaction between A and B, and the TOC measurement includes residual black liquor organics plus the degradation by-products.

The main effects plot (Figure 3.3a) shows the mean percent TOC removed for each factor. The data indicates the black liquor concentration has an overall negative impact on the response, while the TiO$_2$ concentration exhibits an overall positive effect. A larger vertical displacement for black liquor concentration indicates that the black liquor concentration shows a greater magnitude of effect than the TiO$_2$ concentration. The interaction plot (Figure 3.3b) can assess the interaction effect between the experimental factors through the slope of the line. Non-parallel lines in the interaction plot indicate a high degree of interaction, where a slightly positive effect by the TiO$_2$ concentration was observed at high black liquor concentrations while a strongly positive effect by the TiO$_2$ concentration was observed at low black liquor concentrations. This is shown by a steeper slope at the low-level black liquor concentration. Eventually, the main effect of each factor and the interaction effect were qualified, and an ANOVA was performed to verify the effect significance.

a)

b)
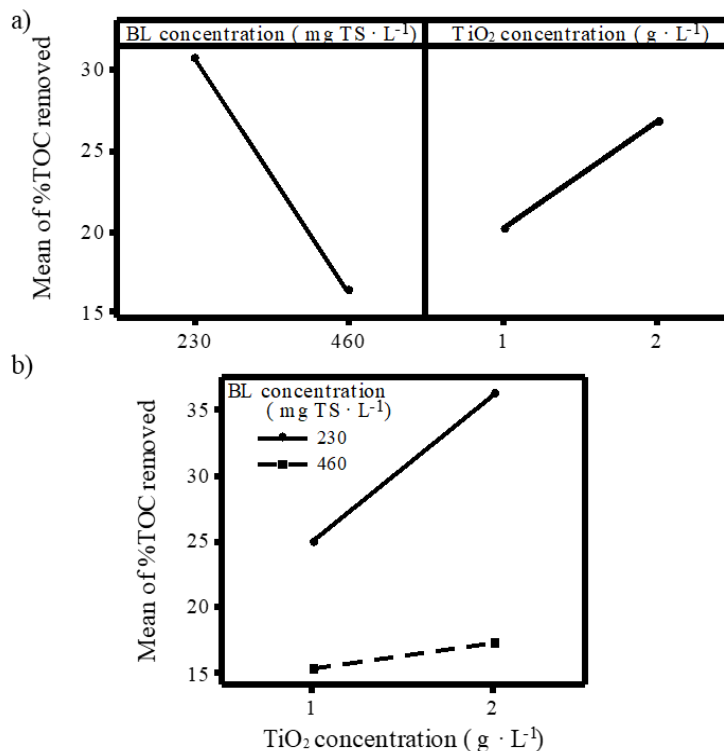
Figure 3.3 (a) Main effects and (b) Interaction plots.
Note: BL = Black liquor, the TOC measurement includes residual black liquor organics plus the degradation by-products, each point represents the mean value of all points at each level, and the deviation for a factor at one level is expressed as $dev_{factor(level)}$, $dev_{BL(low)} = 6.7$, $dev_{BL(high)} = 2.4$, $dev_{TiO_2(low)} = 5.7$, $dev_{TiO_2(high)} = 11.1$.

3.3.3. ANOVA analysis

The result of ANOVA by Minitab (Table 3.3) indicates that the black liquor concentration has a negative effect on the TOC removal, while TiO_2 concentration has a positive effect. A positive effect can also be observed for the combination of high black liquor concentration and low TiO_2 concentration or the combination of low black liquor concentration and high TiO_2 concentration. The percent contribution is the percent contribution of each term's sum of squares (SS) relative to the total SS. This is a useful guide to the relative importance of every model term [8]. In this study, the black liquor concentration dominated the process and accounted for over 70% of the total variability.

In comparison, the TiO_2 concentration and interaction effect accounted for 16% and 8%, respectively. The P-values are used to confirm the magnitude of the effects. As shown in Table 3.3, none of the terms has a p-value larger than 0.05. This indicated the significant effects of the black liquor concentration, the TiO_2 concentration and their interaction on the percent TOC removed.

Table 3.3 Effects estimation and ANOVA for each factor.

Term	Effect	Sum of Squares	Percent Contribution	P-Value
Black liquor concentration	-14.3	409.0	76%	0.001
TiO_2 concentration	6.60	87.12	16%	0.015
Black liquor $\times$ TiO_2 concentration	-4.65	43.25	8%	0.046

In conclusion, the selected factors, black liquor concentration, and TiO_2 concentration will impact the TOC reduction significantly. Hence, the effect of these two factors combination cannot be neglected. Based on this study, the black liquor concentration at 230 mg $TS \cdot L^{-1}$ and the TiO_2 concentration at 2 $g \cdot L^{-1}$ are the optimum condition for maximizing the percent TOC removed from diluted black liquor.

3.4. References

[1] S. N. Vadodaria, Effect of black liquor on the activated sludge process: An experimental investigation of the effect of black liquor on the activated sludge treatment of bleached kraft mill effluents, Thesis, McGill University, 1999.

[2] L. Cai, Q. Long, C. Yin, Synthesis and characterization of high photocatalytic activity and stable Ag_3PO_4/TiO_2 fibers for photocatalytic degradation of black liquor, Appl. Surf. Sci. 319 (2014) 60–67.

[3] R. Prado, X. Erdocia, J. Labidi, Effect of the photocatalytic activity of TiO_2 on lignin depolymerization, Chemosphere 91 (2013) 1355–1361.

[4] P. Peralta-Zamora, S.G.D. Moraes, R. Pelegrini, M. Freire, J. Reyes, H. Mansilla, N. Durán, Evaluation of ZnO, TiO_2 and supported ZnO on the photoassisted remediation of black liquor, cellulose and textile mill effluents, Chemosphere 36 (1998) 2119–2133.

[5] W.A. Shewa, Converting low value lignocellulosic residues into valuable products using photo and bioelectrochemical catalysis, in: J. Lalman (Ed.), Ph.D. Thesis, University of Windsor, 2016.

[6] S. Ray, J.A. Lalman, N. Biswas, Using the Box-Benkhen technique to statistically model phenol photocatalytic degradation by titanium dioxide nanoparticles, Chem. Eng. J. 150 (2009) 15–24.

[7] J.A. Lalman, W.A. Shewa, Microbial fuel cell for generating electricity, and process for producing feedstock chemicals, US20160064758A1, 2016.

[8] D.C. Montgomery, The 2^k factorial design, in: D.C. Montgomery (Ed.), Design and analysis of experiments, John Wiley and Sons, Inc., Hoboken, 2012, pp. 752.

[9] Minitab, Inc., Effects plots for analyze response surface design,

https://support.minitab.com/en-us/minitab/18/help-and-how-to/modeling-

statistics/doe/how-to/response-surface/analyze-response-surface-design/interpret-the-

results/all-statistics-and-graphs/effects-plots/ (accessed July 15, 2019).

CHAPTER 4

OPTIMIZING THE BLACK LIQUOR PHOTODEGRADATION USING THE RESPONSE SURFACE METHODOLOGY

4.1. Introduction

Black liquor is the spent liquor from the Kraft and other pulping process. Traditionally, black liquor is burned in energy recovery boilers after evaporation. From the perspective of energy, a recovery boiler can reach high thermal efficiencies varying between 66% and 75% based on the percent solids in black liquor [1]. However, from the perspective of the environment, recovery boilers release highly volatile fugitive air contaminants to the atmosphere, including particulate matter, sulfur dioxide, and reduced sulfur compounds [2]. In addition, some organic chemicals in pulp and paper mill wastes are toxic and persistent chemicals, especially chlorolignins and chlorophenols [3]. These environmental challenges are driving the pulp and paper industry to apply various approaches as environmentally-friendly alternatives, such as black liquor gasification [4], membrane filtration [5], ozone treatment [6], and photocatalysis [3].

Recently, photocatalysis has become a promising treatment as an AOP because photocatalysis is cleaner and more effective, energy efficient, and economical. The strong oxidant species produced from photocatalysis, such as $\bullet OH$ and $\bullet O_2^-$, are able to oxidize almost all organic pollutants. This is expected to improve the degradability and reduce the toxicity of pulp and paper mill wastes [7]. For example, during photocatalysis of lignin, the short-chain organic acids and malonic acid which are produced are eventually converted to CO_2 [8]. With regard to toxicity reduction, Peralta-Zamora et al. [3] used

TiO_2/ZnO and UV irradiation to examine the impact of photochemical treatment of black liquor toxicity reduction. These researchers reported approximately a 50% of toxicity reduction, accompanied with approximately 50% mineralization to CO_2. In a similar study conducted by Yeber et al. [7] on pulp and paper bleaching wastes, significant detoxification was achieved by TiO_2 photocatalysis.

The efficiency and by-products of the photocatalytic degradation process is dependent on factors such as the catalyst type and concentration, the substrate concentration, the pH, reaction temperature, light intensity, ionic components in solution, mixing rate, and oxidizing agents/electron acceptors [9]. To optimize these parameters, a variety of studies have examined the impact of each factor on the photocatalysis. For example, a smaller particle size of TiO_2 leads to a more active photocatalytic reaction due to a larger SSA, especially for the particles smaller than 30 nm [10]. In the present study, the particle size of TiO_2 was selected in the range from 5 nm to 25 nm for investigating the effect of particle size below 30 nm on the percent TOC removed. Moreover, a higher temperature increases the reactivity of photocatalysis, but under these conditions, the lower dissolved oxygen level leads to reduced photocatalytic rates [11]. The effect of temperature on the photocatalytic degradation of phenol at 23 °C, 30 °C, and 37 °C was reported by Choquette-Labbé et al. [12]. These researchers reported the operating temperature of 37 °C combined with 10 nm TiO_2 particles achieved the optimal degradation of phenols. In the present study, the temperature was selected in the range from 23 °C to 37 °C for investigating the interaction effects between temperature and other two factors by using BBD.

The effect of pH on photocatalysis has been under debate because both acidic [13] and alkaline [14] conditions are able to attain a high photocatalytic reactivity of lignin.

Interaction effects between the substrate concentration and pH or between pH and the TiO_2 concentration could play a major role in explaining the impact of pH on photocatalytic degradation of lignin [15]. In the present study, the pH was selected in the range from 5 to 9 for investigating whether acidic or alkaline condition can achieve a higher photocatalytic degradation. Interactions between factors could lead to the misinterpretation of results and hence, is worthwhile to examine the interaction effects.

The BBD was selected for this study because the method can avoid extreme situations, namely, all factors at their highest or lowest levels simultaneously [16]. If the extreme level response prediction is not of interest, BBD would become more efficient and require fewer experiments than other statistical designs, such as central composite design (CCD) [16]. However, compared with FFD, the BBD and CCD approaches are much more efficient, despite being less accurate to some extent.

On the basis of a specific experiment design, RSM can develop a statistical model. This model can investigate the interaction effect between several independent variables on the response and can also simulate a response surface aiming to evaluate the peak or valley response. During the RSM process, a second-order mathematical model is generated using a regression analysis technique. The effect of each factor on the response is reflected by the coefficients in front of each factor, and the significance of multivariate combination can explain the interaction effect on the response. Moreover, a reasonable prediction can also be made by this model as long as the model fits well [17].

In the present study, a BBD was used for optimizing the TOC removal efficiency of black liquor. Three practical factors were selected in this BBD: pH, temperature, and catalyst particle size. Subsequently, RSM was developed based on the measured percent

TOC removed, and an ANOVA was performed for model evaluation. Finally, a D-optimality analysis determined the optimal set of the selected factors and was accompanied by the response surface plot for the optimal conditions.

4.2. Materials and methods

4.2.1. Statistical design: Box-Behnken design

For the optimal TOC removal, 230 mg TS·L^{-1} black liquor and 2 g·L^{-1} TiO$_2$ were used as the initial composition based on the results of the study in Chapter 3. To degrade recalcitrant components in black liquor, such as lignin, Lalman et al. [18] determined that the irradiation time should be 4 hours. Therefore, the current study will use a four-hour irradiation time.

A three-level, three-factor BBD was applied for the optimization of the TOC removal efficiency of black liquor. In consideration of practicality, an initial pH ranging from 5 to 9 [15], a temperature ranging from 23 °C to 37 °C [12], and a particle size ranging from 5 nm to 25 nm [10] were sequentially denoted by X_1, X_2, and X_3 for this optimization study. In addition, each of these unencoded independent variables was coded at a center level (0), low level (-1), and high level (+1). The value of each variable could be determined by the following transformation (Eq. (4.1)) [19]:

$$x_i = (X_i - X_0)/\Delta X_i \qquad (4.1)$$

where x_i is the code level of the ith variable, X_0 is the center point of the uncoded ith independent variable, X_i is the uncoded value of the ith variable at each code level, and ΔX_i are the step change values. Table 4.1 shows the input values of the three different factors:

initial pH, temperature, and catalyst particle size.

Table 4.1 Box-Behnken design parameters [10, 12, 15].

Factors	Model Terms	Low (-1)	Central (0)	High (+1)	$\Delta X_i{}^a$
pH	X_1	5	7	9	2
Temperature (°C)	X_2	23	30	37	7
TiO$_2$ particle size (nm)	X_3	5	15	25	10

[a] Step change values.

Based on the characteristics of BBD, all factors with three-levels were correspondingly placed at the center and the midpoints of the edges of the box. Thus, the BBD is advantageous because the BBD is developed using 15 experimental points: twelve (#1 – #12) on the edges and three (#13 – #15) in the center, and they are all spherical and rotatable designs. The BBD requires fewer experiments than the FFD of 27 experiments with three factors. The center points were triplicated, designated as #13, #14 and #15, operating under the same experimental conditions to estimate the experimental error. In total, 15 batch experiments were conducted under specific conditions and tabulated (Table 4.2). Besides, all 15 experimental conditions were conducted in triplicate.

Table 4.2 BBD matrix.

Exp. #	Initial pH of the solution		Temperature (°C)		Particle size (nm)	
	x1 (coded)	X1 (uncoded)	x2 (coded)	X2 (uncoded)	x3 (coded)	X3 (uncoded)
1	+1	9	+1	37	0	15
2	0	7	-1	23	+1	25
3	0	7	+1	37	+1	25
4	+1	9	-1	23	0	15
5	+1	9	0	30	-1	5
6	+1	9	0	30	+1	25
7	0	7	-1	23	-1	5
8	-1	5	+1	37	0	15
9	0	7	+1	37	-1	5
10	-1	5	-1	23	0	15
11	-1	5	0	30	+1	25
12	-1	5	0	30	-1	5
13	0	7	0	30	0	15
14	0	7	0	30	0	15
15	0	7	0	30	0	15

Table 4.2 shows that within the boundary condition, there was no experimental conditions whose factors occurred at high or low levels simultaneously. Moreover, BBD allows for the development of optimization models to determine the linear effects of the factors, and to assess the multivariate effects on the response [16].

4.2.2. Chemicals

Black liquor was obtained from a pulp and paper mill located in Lakehead, Ontario, Canada. After weighing the TiO_2 and adding it to Milli-Q® water, the stock suspensions of TiO_2 nanoparticles were prepared and stored at 23 ± 2 °C in 100 mL serum bottles. The TiO_2 stock solutions were sonicated using an ultrasonic bath produced from VWR (Mississauga, Ontario) for 15 to 20 minutes to ensure thorough mixing prior to the

preparation of reaction solutions. This process produced a homogeneous suspension that was used to deliver a more accurate quantity of catalyst to the diluted black liquor solution.

4.2.3. Photocatalysis

The mixture volume contained in each quartz tube was 50 mL: 40 mL Milli-Q® water, 5 mL TiO_2 solution, and 5 mL black liquor solution. The photodegrading experiments were conducted using the photoreactor configuration described in Chapter 2 (Section 2.3.1). The reaction mixtures were placed into the photoreactor. The temperature-controlled system and cooling fan were used to maintain the photoreactor at the desired temperature.

4.2.4. pH adjustment

To ensure that the desired pH was accurately achieved in each solution, the pH of the reaction solutions was adjusted before photocatalysis using a pH meter (VWR, Mississauga, Ontario), HCl (37% w/w), and NaOH (97% purity), which were purchased from Fisher Scientific (Ontario, Canada). All solutions were prepared and mixed using Milli-Q® water.

4.2.5. Sampling and analytical methods

4.2.5.1. Sample collected

The samples were collected under 4h irradiation conditions, at 1h time intervals. The samples were diluted, and the TOC content was measured using a TOC-L instrument. The percent TOC removed was set as the response variable of BBD.

4.2.5.2. Response Surface Methodology (RSM)

RSM consists of experimental design, modeling and optimization. In the first step, an appropriate experimental design such as CCD or BBD is chosen based on the features of each design method. Next, an appropriate model is introduced to describe the true relationships between factors and their responses during the modeling step. Finally, the optimization step can determine the optimal set of factors based on one or more responses.

An RSM model of the experimental factors (x_1, x_2, and x_3) and percent TOC removed (Y) was developed using Minitab 18 (Minitab Inc., State College, Pennsylvania). In this model, x_1 represents the initial pH, x_2 represents the temperature of the synthesis, and x_3 represents the photocatalyst particle size. RSM can create a regression model based on all measured responses and can generate a response surface. The response surface is commonly presented in a quadratic equation (Eq. (4.2)) [19]:

$$Y = \beta_0 + \sum_{i=1}^{k} \beta_i x_i + \sum_{i=1}^{k} \beta_{ii} x_i{}^2 + \sum_{i=1}^{k}\sum_{j=1}^{k} \beta_{ij} x_i x_j + \varepsilon \qquad (4.2)$$

where Y is the measured response or result of experiments, i and j are the index numbers of each pattern, k is the number of patterns, β_0 is the intercept term, β_i is the linear coefficient of the corresponding coded variables, β_{ii} is the square coefficient of the corresponding coded variables, β_{ij} is the interaction coefficient between the ith and j^{th} variables, x_1, x_2,…, x_k are coded variables, and ε is the error that includes measurement error.

The three variables involved in this study included pH, temperature, and catalyst particle size, setting k = 3. Based on the experimental results from the BBD study, there are 45 TOC removal efficiencies for three experimental replicates, which were determined by the

TOC-L instrument. These results were used as input parameters to estimate the RSM model (Table 4.3). Table 4.3 shows that the input of the RSM under the percent TOC removed at 4-hour was set as the response (Y).

Subsequently, an ANOVA was used to identify significant terms in the final model of RSM. If the p-values of the variables' coefficients calculated by ANOVA are less than 0.05, the effect of the corresponding factors on response is considered statistically significant and cannot be omitted. Other statistical analysis using Minitab included the D-optimality index and the Anderson-Darling (AD) statistic. The D-optimality analysis can assist in determining an optimum design to maximize the percent TOC removed in this study [20]. In addition, the AD statistic is able to test whether the residuals are fitting to a normal distribution [20].

4.3. Results and discussion

4.3.1. Statistical summary and analysis

The percent TOC removed for each condition of BBD is determined based on the initial TOC and final TOC values. The confidence intervals for the mean values at a 95% confidence level were calculated and summarized for each condition (Table 4.3). All data analyses were based on experimental conditions with three replicates.

Table 4.3 Percent TOC removed at different factor levels.

Exp. #	pH	Temperature (°C)	Particle size (nm)	TOC removed (%)
1	9	37	15	38.7±2.3
2	7	23	25	35.6±3.2
3	7	37	25	38.0±2.1
4	9	23	15	26.1±3.5
5	9	30	5	40.2±1.6
6	9	30	25	42.9±2.2
7	7	23	5	40.6±0.6
8	5	37	15	25.3±3.9
9	7	37	5	49.5±3.6
10	5	23	15	10.9±3.0
11	5	30	25	19.5±2.7
12	5	30	5	35.0±0.8
13	7	30	15	24.1±2.0
14	7	30	15	24.4±2.6
15	7	30	15	25.5±2.8

Note: The TOC measurement includes residual black liquor organics plus the degradation by-products.

The values of percent TOC removed varied with different conditions, ranging from 10.9±3.0% to 49.5±3.6%. The maximum percent TOC removed was achieved by #9 experiment, namely, a pH of 7, 37 °C and a TiO_2 particle size of 5 nm. In contrast, a larger particle size (25 nm) in #3 experiment or a lower temperature (23 °C) in #7 experiment achieved a slightly smaller percent of TOC removed, as shown in Figure 4.1. These results suggest that a higher temperature and smaller TiO_2 particles are preferable.
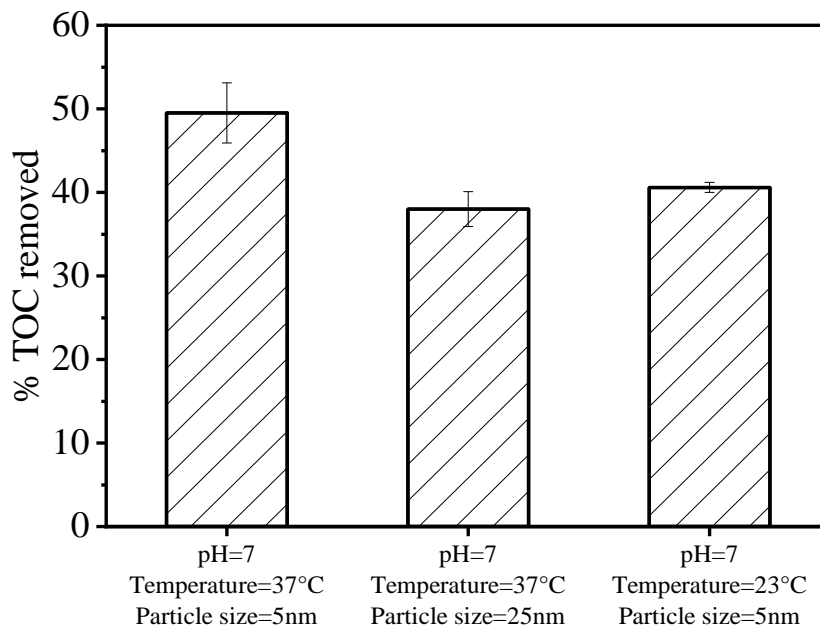
Figure 4.1 TOC reductions under three conditions at pH = 7.
Note: The TOC measurement includes residual black liquor organics plus the degradation by-products.

4.3.2. *Main effects plot and interaction plots*

The main effects plot was used to examine each factor's impact, which reflects the mean response value at each factor level [21]. In Figure 4.2, the increase in temperature and pH shows an overall positive effect on TOC removal. A low-level pH (pH = 5) is linked to the lowest percent TOC removed, whereas a small particle size (5 nm) is linked to the highest percent TOC removed. Compared with pH and temperature, a larger vertical displacement was observed when the particle size varied. The data indicate that the particle size has a greater effect on percent TOC removed.
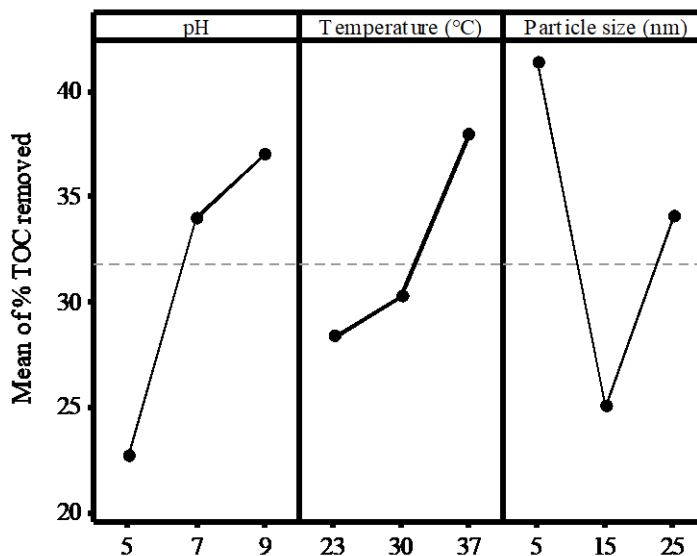
Figure 4.2 Main effects plots.
Note: The TOC measurement includes residual black liquor organics plus the degradation by-products, each point represents the mean value of all points at each level, and the deviation for a factor at one level is expressed as $dev_{factor(level)}$, $dev_{pH(low)} = 9.4$, $dev_{pH(mid)} = 9.4$, $dev_{pH(high)} = 7.0$, $dev_{tem(low)} = 12.0$, $dev_{tem(mid)} = 8.7$, $dev_{tem(high)} = 9.3$, $dev_{size(low)} = 5.7$, $dev_{size(mid)} = 8.0$, $dev_{size(high)} = 9.4$.

The non-parallel lines in the interaction plots (Figure 4.3) show the interaction between the different factors, and the more non-parallel lines indicate the stronger strength of interaction effect [22]. Accordingly, the interaction effect on the response between pH and particle size could not be neglected because all three lines intersect in the interaction plot between pH and particle size. Despite fewer non-parallel lines in the other interaction plots, their effects require further discussion. Notice that the ANOVA test should be performed to ensure an appropriate estimation on the significance of the interaction effects [22].
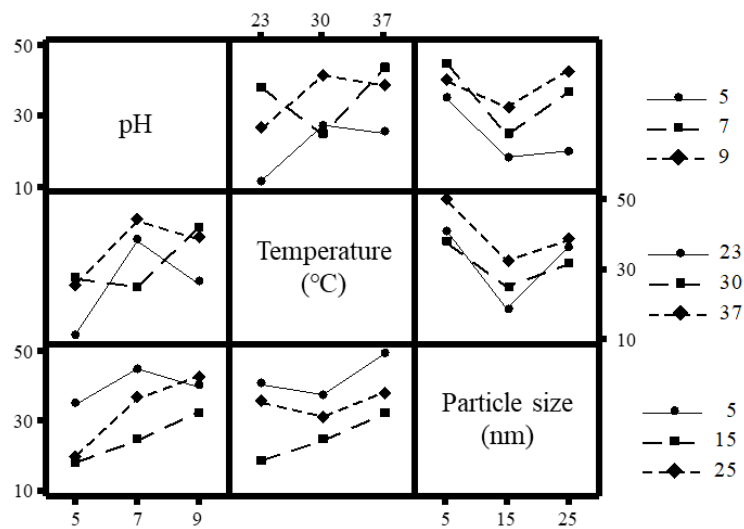
Figure 4.3 Interaction plots.

The normal plot of the effects was selected to compare the statistical significance of linear, square and interaction effects on TOC removal. Points located on or near the straight line indicate zero effect in the normal plot [23]. As shown in Figure 4.4, three factors were denoted by A, B, and C (A = pH, B = temperature, and C = particle size). All the effects except AB are significant at a confidence level of 95% ($\alpha = 0.05$). Hence, there were no interaction effects on TOC removal between pH and temperature, which was consistent with the results of Soares et al. [24]. Except for the interaction effects between pH and temperature, all the other terms are statistically significant, including the linear, square and remaining interaction terms. In addition, the increase in C, AA, and BC can have a negative impact on TOC removal efficiency because these terms are located on the left side of the straight line [23]. In contrast, the terms on the right side of the straight line, such as CC or BB, show positive effects on the response.
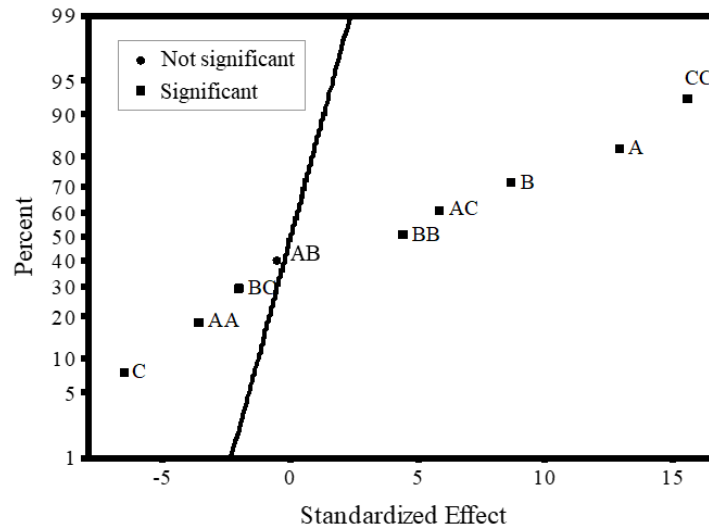
Figure 4.4 Normal plot of the factorial linear, square and interaction effects.
Note: A = pH, B = Temperature, C = Particle size, and AB, BC, AC = Interaction effects.

4.3.3. Response surface model development

The ANOVA is a statistical analysis method that evaluates the model's adequacy and interprets the factorial effects on the response in the full quadratic model. The ANOVA (Table 4.4) of the TOC removal efficiency illustrates that this model is statistically significant because of p-value < 0.05 [25]. The F-value of the model was 66.3, which was much higher than the F-critical value of 2.16 (df1 = 9, df2 = 35, α = 0.05), indicating that this model was significant [26]. The insignificant interaction effect between pH and temperature on the response was verified because the p-value was larger than 0.05. In contrast, the interaction effects between pH and particle size, and between temperature and particle size were verified and had p-values < 0.05.

Table 4.4 ANOVA for factorial linear, square and interaction effects.

Source	DF[a]	Adj SS[b]	Adj MS[c]	F-Value	P-Value
Model	9	4437	493.0	66.26	0.000
Linear	3	2098	699.3	93.98	0.000
pH	1	1228	1228	165.1	0.000
Temperature	1	549.1	549.1	73.80	0.000
Particle size	1	320.5	320.5	43.07	0.000
Square	3	2054	684.7	92.01	0.000
pH*pH	1	98.40	98.40	13.22	0.001
Temperature*Temperature	1	140.5	140.5	18.88	0.000
Particle size*Particle size	1	1787	1787	240.2	0.000
2-Way Interaction	3	285.1	95.04	12.77	0.000
pH*Temperature	1	2.520	2.520	0.340	0.564
pH*Particle size	1	250.3	250.3	33.63	0.000
Temperature*Particle size	1	32.34	32.34	4.350	0.044
Error	35	260.4	7.440		
Total	44	4697			

Note: [a] DF = degrees of freedom, [b] Adj SS = adjusted sum of squares, [c] MS = mean square.

To generate a fitted RSM model for TOC removal, the backward elimination method was performed to simplify the full quadratic model. The backward elimination method considers all the potential terms first and removes one insignificant term for every step until all the remaining terms are significant [27]. Using this approach, this model is advantageous for considerable predictive capability. In this study, all the variables and responses were fitted to a refined quadratic model (Eq. (4.3)), that had an F-value of 75.9, which was greater than F-critical (2.2 for $df1 = 8$, $df2 = 36$, and $\alpha = 0.05$). The data indicate the significance of this refined quadratic model.

$$Y = 55.5 + 10.58A - 3.33B - 5.07C - 0.745A^2 + 0.073B^2 + 0.127C^2 + 0.228\ AC$$

$$- 0.024\ BC \hspace{4cm} (4.3)$$

where Y is the TOC removal (%), A represents the initial pH, B represents the temperature (°C), and C represents the TiO$_2$ particle size (nm).

4.3.4. Response surface and contour plots

According to the predictive model from Minitab, two-dimensional contour plots were embedded into three-dimensional surface plots using MATLAB (MathWorks, Natick, Massachusetts), as shown in Figures 4.5, 4.6 and 4.7. These combined plots show how the response surfaces vary with the factors and directly identify the location of the maximum TOC removal and the corresponding set of factor values. The iso-lines in each contour plot were labeled at intervals of 5, which illustrates the distribution of the response surface gradient.

The response surface under the dimensions of pH and temperature was plotted in Figure 4.5, which shows the percent TOC removed raised along the diagonal, and the maximum percent TOC removed value was achieved at a pH of 9 and at 37 °C. The gradient in the ascending direction of the diagonal was relatively uniform due to the absence of interaction disturbance between pH and temperature.
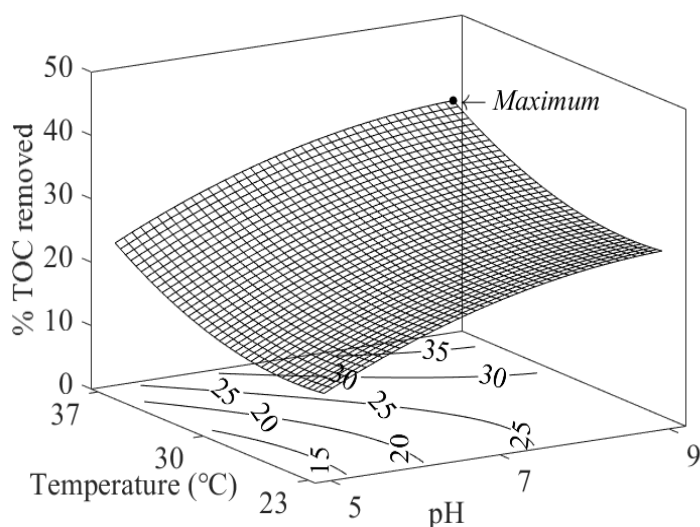
Figure 4.5 Response surface plot of pH and temperature at the 15 nm particle size. Note: The TOC measurement includes residual black liquor organics plus the degradation by-products.

The response surface under the dimensions of pH and particle size is plotted in Figure 4.6. A clear valley can be observed at 15 nm TiO_2, illustrating the negative effect of TiO_2 with a particle size of approximately 15 nm on TOC removal efficiency. This effect was consistent with the result of Carbeiro et al. [28]. These researchers reported that TiO_2 particles at 15 nm showed a minimum of photocatalytic activities within a particle size range of 7 to 35 nm. They attributed the decrease in photocatalytic activity to the decline of OH-groups within the size range of 7 to 15 nm [28]. In addition, the maximum percent TOC removed was estimated at a pH of 9 and a TiO_2 particle size of 25 nm. Almquist et al. [29] reported that 25 nm TiO_2 particles exhibited the most apparent photoactivity in the range of 25 to 40 nm. In addition, a greater photocatalytic activity was observed when the particle size increased or decreased from 15 nm. Moreover, increasing particle size can obtain a more effective increase in percent TOC removed than decreasing particle size at high-level pH values at 30 °C.
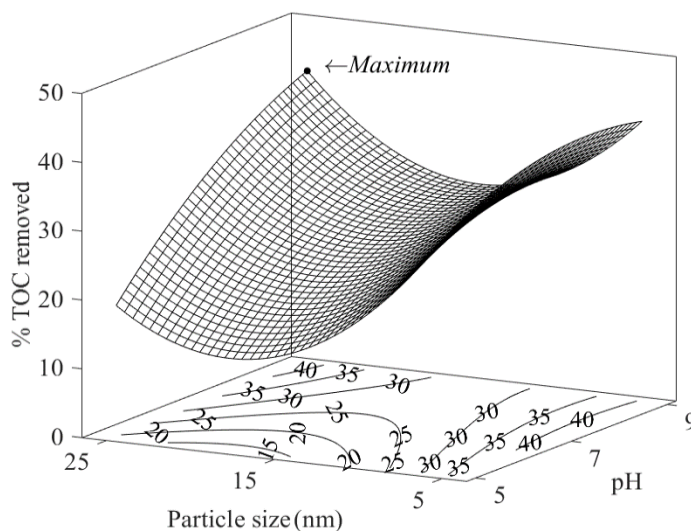
Figure 4.6 Response surface plot of pH and particle size at 30 °C.
Note: The TOC measurement includes residual black liquor organics plus the degradation by-products.

The response surface under the dimensions of temperature and particle size was demonstrated in Figure 4.7. This response surface is characterized by a concave area around the center. The iso-lines are in a quasi-circular pattern due to the dominance of the positive square terms of these two factors. In addition, the concentric contour illustrates the location of a minimum response point, which was at approximately 15 nm of particle size and 25 °C. A larger response can be observed at the points farther away from the lowest response. The maximum percent TOC removed was observed at 5 nm TiO_2 and 37 °C because of the interaction effect between the temperature and catalyst particle size on TOC removal efficiency.
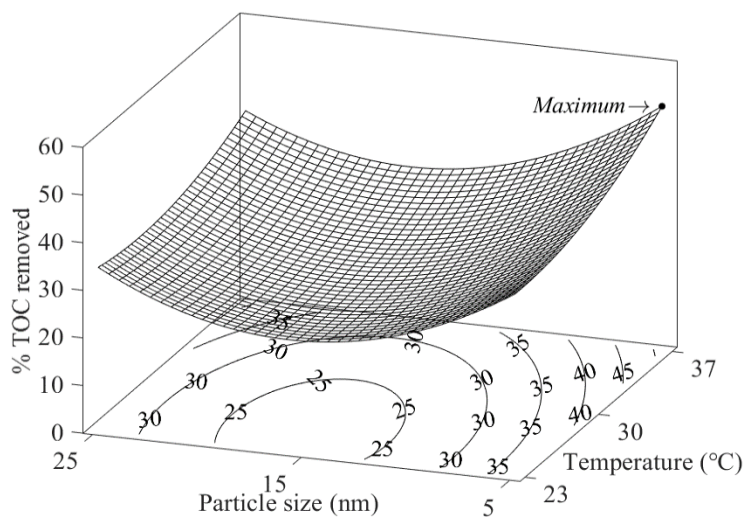
Figure 4.7 Response surface plot of TiO$_2$ particle size and temperature at pH = 7. Note: The TOC measurement includes residual black liquor organics plus the degradation by-products.

4.3.5. Verification of the response model and optimization

The regression coefficient R-squared value of 94.4% for Eq. (4.3) demonstrates that the model can describe 94.4% of the variation of the measured TOC removal efficiency, so this model has a reasonable fit with the observations. The predicted R-squared value of 91.2% indicates the accurate predictive ability of this refined model.

The residuals were calculated using Minitab to determine the difference between the experimental results and the corresponding predicted values. The residuals plotted with the experiment order are shown in Figure 4.8. Note the experimental order is the same as in Table 4.3 with three replicates. This plot shows that the residuals are varied around the center line randomly, so the residuals are not dependent on the experimental order [30].
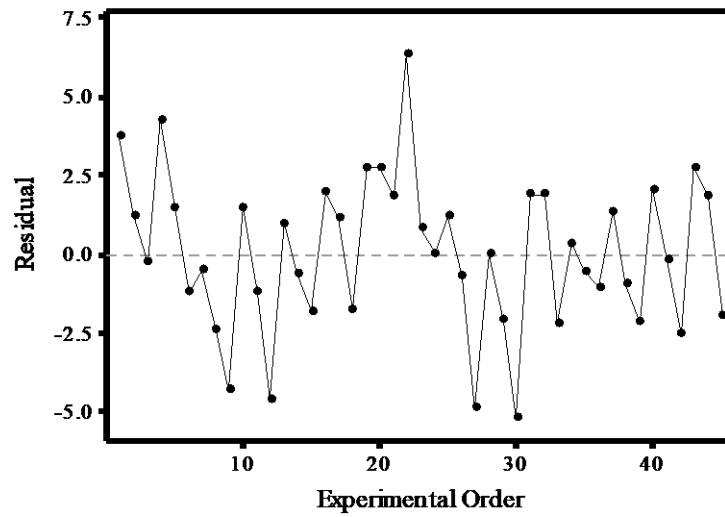
Figure 4.8 Residuals versus experimental order plot.

To estimate whether the residuals follow the normal distribution, the AD statistic was performed and the results shown in Figure 4.9. The observed AD value (0.314) was less than the critical AD value (0.738) in the case of a sample size of 45 at a 95% confidence level. The p-value (0.533) above 0.05 further confirmed that the residual distribution followed the normal distribution [31, 32].
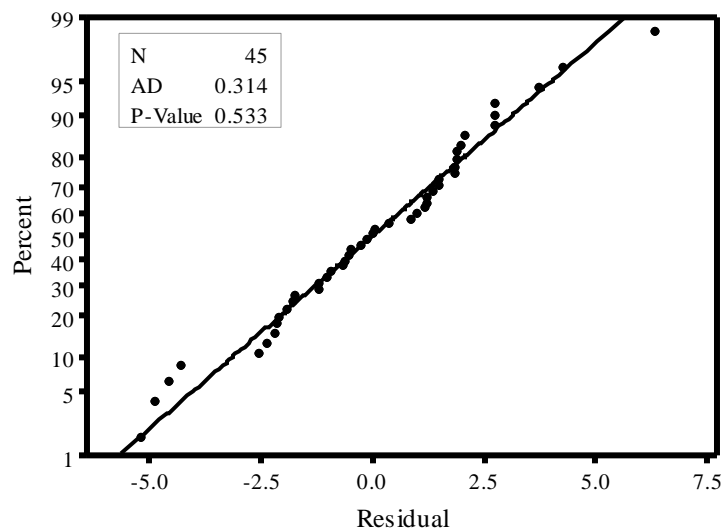

Figure 4.9 AD normality plot.

The D-optimality was used to locate the maximum percent TOC removed. In this study, the D-optimality result (Figure 4.10) was generated using the response optimizer function in Minitab software. The D-optimality provides a D index to explain the extent to which the combination of optimal factor values achieves the goal of maximizing the percent TOC removed, and the D value varies between 0 (undesirable) and 1 (ideal) [33]. The curve in each cell shows how the percent TOC removed varies with the corresponding factor, when the other two factors remain at their optimal values [34]. In each cell, the y-axis represents the percent TOC removed, and the x-axis represents each factor. The maximum percent TOC removed (51.6%) was determined by the largest D-optimality index (0.986) and predicted by the fitted model under the conditions of a pH of 7.87, 37 °C, and a TiO_2 particle size of 5 nm. Three surface plots at the optimum factor values (Figure 4.11) indicate the location of maximum responses in the corresponding spaces. In this case, an overall elevation of response surfaces in each space was observed compared to the mid-level surface plots. This indicates that using any optimal factorial value can improve efficiency.

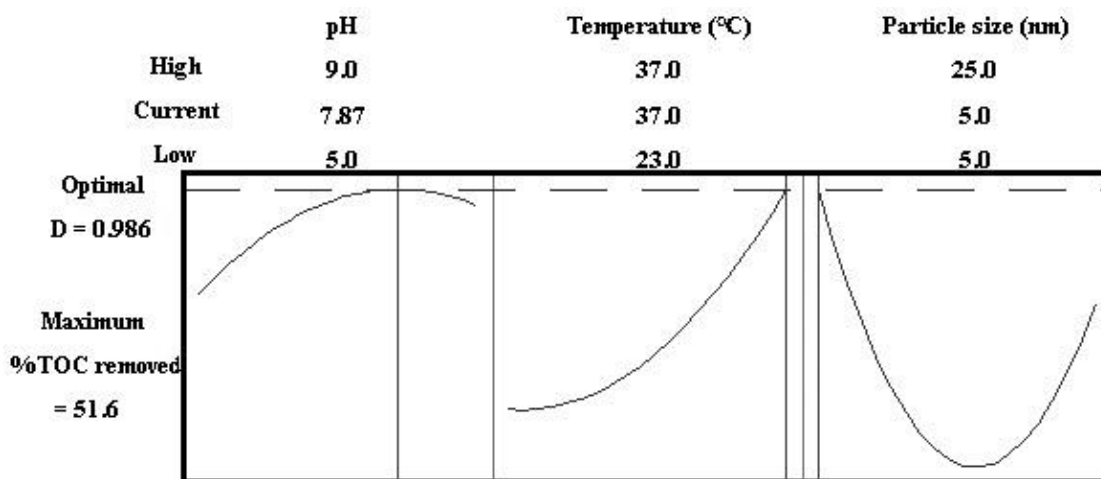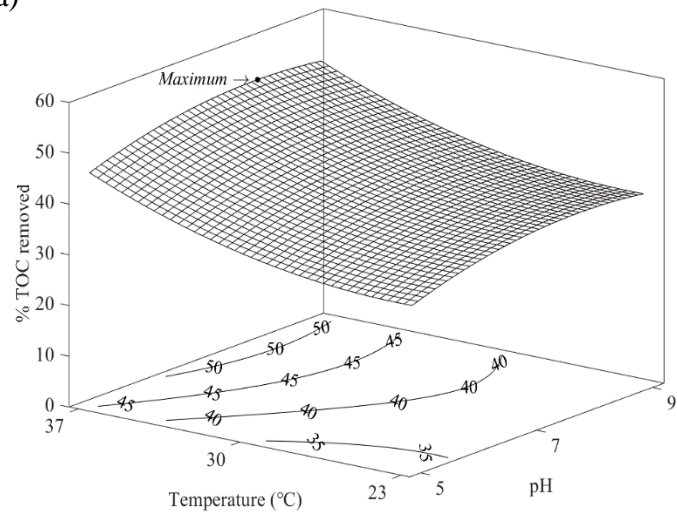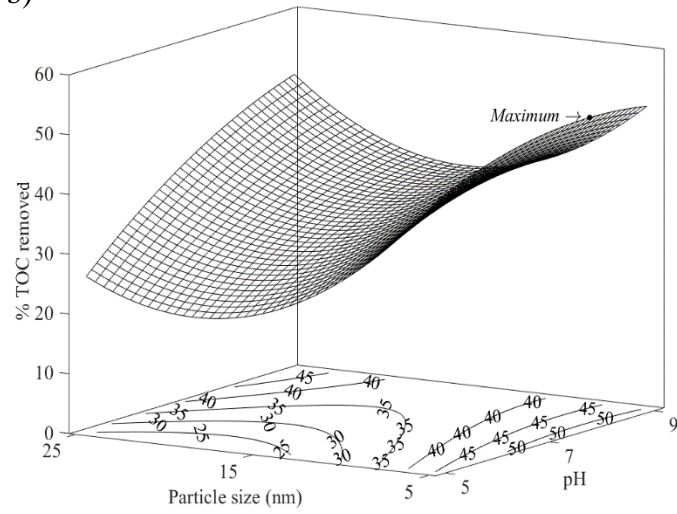|	pH	Temperature (°C)	Particle size (nm)
High	9.0	37.0	25.0
Current	7.87	37.0	5.0
Low	5.0	23.0	5.0

Figure 4.10 D-optimality plot for maximizing TOC removal efficiency.
Note: The TOC measurement includes residual black liquor organics plus the degradation by-products.

a)

b)

c)
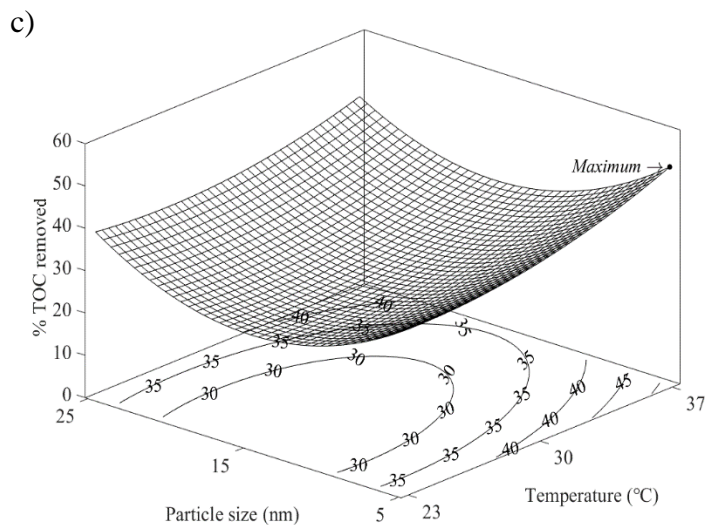
Figure 4.11 The optimum TOC removal point at a) pH = 7.87, b) 37 °C, and c) 5 nm. Note: The TOC measurement includes residual black liquor organics plus the degradation by-products.

In conclusion, the RSM provided a reasonable estimation within the selected range of each factor. According to the model in RSM, the percent TOC removed from black liquor has no interaction effect between pH and temperature. The maximum TOC removal efficiency was calculated be achieved under the conditions of a pH of 7.87, 37 °C, and a TiO$_2$ particle size of 5 nm. Moreover, the 15 nm catalyst was not recommended because of low photocatalytic performance.

4.4. References

[1] J. Porter, T. Sands, T. Trung, Understanding the kraft liquor cycle: A need for online measurement and control, Tappi Engineering, 2009.

[2] Environment and Climate Change Canada, Code of practice for the management of air emission from pulp and paper mills, (2016). https://www.canada.ca/en/environment-climate-change/services/canadian-environmental-protection-act-registry/guidelines-objectives-codes-practice/issuance-statement-pulp-paper-facilities/code-practice-pulp-paper-facilities.html (accessed July 17, 2019).

[3] P. Peralta-Zamora, S.G. Moraes, R. Pelegrini, M. Freire, J. Reyes, H. Mansilla, N. Durán, Evaluation of ZnO, TiO_2 and supported ZnO on the photoassisted remediation of black liquor, cellulose and textile mill effluents, Chemosphere 36 (1998) 2119–2133.

[4] M. Naqvi, J. Yan, E. Dahlquist, Black liquor gasification integrated in pulp and paper mills: A critical review, Bioresource Technol. 101 (2010) 8001–8015.

[5] A. Arkell, J. Olsson, O. Wallberg, Process performance in lignin separation from softwood black liquor by membrane filtration, Chem. Eng. Res. Des. 92 (2014) 1792–1800.

[6] K.S. Ng, J.C. Mueller, C.C. Walden, Ozone treatment of kraft mill wastes, J. Water Pollut. Control Fed. 50 (1978) 1742–1749.

[7] M.C. Yeber, J. Rodríguez, J. Freer, N. Durán, H. D. Mansilla, Photocatalytic degradation of cellulose bleaching effluent by supported TiO_2 and ZnO, Chemosphere 41 (2000) 1193–1197.

[8] K. Kamwilaisak, P.C. Wright, Investigating laccase and titanium dioxide for lignin degradation, Energ. Fuel. 26 (2012) 2400–2406.

[9] S. Ahmed, M.G. Rasul, W.N. Martens, R. Brown, M.A. Hashib, Advances in heterogeneous photocatalytic degradation of phenols and dyes in wastewater: A review, Water Air Soil Poll. 215 (2011) 3–29.

[10] N. Xu, Z. Shi, Y. Fan, J. Dong, J. Shi, M.Z.C. Hu, Effects of particle size of TiO_2 on photocatalytic degradation of methylene blue in aqueous suspensions, Ind. Eng. Chem. Res. 38 (1999) 373–379.

[11] J. Villaseñor, H.D. Mansilla, Effect of temperature on kraft black liquor degradation by ZnO-photoassisted catalysis, J. Photoch. Photobio. A 93 (1996) 205–209.

[12] M. Choquette-Labbe, W.A. Shewa, J.A. Lalman, S.R. Shanmugam, Photocatalytic degradation of phenol and phenol derivatives using a nano-TiO_2 catalyst: Integrating quantitative and qualitative factors using response surface methodology, Water 6 (2014) 1785–1806.

[13] C.N. Chang, Y.S. Ma, G.C. Fang, A.C. Chao, M.C. Tsai, H.F. Sung, Decolorizing of lignin wastewater using the photochemical UV/TiO_2 process, Chemosphere 56 (2004) 1011–1017.

[14] S.K. Kansal, M. Singh, D. Sud, Studies on TiO_2/ZnO photocatalysed degradation of lignin, J. Hazard. Mater. 153 (2008) 412–417.

[15] E. Shoko, J.C.D. Costa, E.T. White, Optimization of the reaction rate in the photocatalytic degradation of sodium lignosulfonate in a TiO_2 slurry reactor: A multivariate study with response surface analysis, Dev. Chem. Eng. Min. Process. 12 (2004) 475–489.

[16] S.L.C. Ferreira, R.E. Bruns, H.S. Ferreira, G.D. Matos, J.M. David, G.C. Brandão, E.G.P. Silva, L.A. Portugal, P.S. Reis, A.S. Souza, W.N.L. Santos, Box-Behnken design:

An alternative for the optimization of analytical methods, Anal. Chim. Acta 597 (2007) 179–186.

[17] R.H. Myers, D.C. Montgomery, C.M.Anderson-Cook, Response surface methodology: Process and product optimization using designed experiments, John Wiley and Sons, Inc., Hoboken, 2009.

[18] J.A. Lalman, W.A. Shewa, Microbial fuel cell for generating electricity, and process for producing feedstock chemicals, US20160064758A1, 2016.

[19] K. Yetilmezsoy, S. Demirel, R.J. Vanderbei, Response surface modeling of Pb(II) removal from aqueous solution by Pistacia vera L.: Box-Behnken experimental design, J. Hazard. Mater. 171 (2009) 551–562.

[20] S.R. Shanmugam, S.R. Chaganti, J.A. Lalman, D.D. Heath, Statistical optimization of conditions for minimum H_2 consumption in mixed anaerobic cultures: Effect on homoacetogenesis and methanogenesis, Int. J. Hydrogen Energ. 39 (2014) 15433–15445.

[21] Minitab, Inc., What is a main effects plot?, https://support.minitab.com/en-us/minitab/18/help-and-how-to/modeling-statistics/anova/supporting-topics/basics/what-is-a-main-effects-plot/ (accessed July 15, 2019).

[22] Minitab, Inc., Interpret the key results for interaction plot,

https://support.minitab.com/en-us/minitab-express/1/help-and-how-to/modeling-statistics/anova/how-to/interaction-plot/interpret-the-results/ (accessed July 15, 2019).

[23] Minitab, Inc., Effects plots to analyze response surface design,

https://support.minitab.com/en-us/minitab/18/help-and-how-to/modeling-statistics/doe/how-to/response-surface/analyze-response-surface-design/interpret-the-results/all-statistics-and-graphs/effects-plots/ (accessed July 15, 2019).

[24] E.T. Soares, M.A. Lansarin, C.C. Moro, A study of process variables for the photocatalytic degradation of rhodamine B, Braz. J. Chem. Eng. 24 (2007) 29–36.

[25] D.B.F. Filho, R. Paranhos, E.C.d. Rocha, M. Batista, J.A.d. Silva Jr., M.L.W.D. Santos, J.G. Marino, When is statistical significance not significant?, Bras. Political Sci. Rev. 7 (2013) 31–55.

[26] S.S. Veeravalli, S.R. Chaganti, J.A. Lalman, D.D. Heath, Optimizing hydrogen production from a switchgrass steam exploded liquor using a mixed anaerobic culture in an upflow anaerobic sludge blanket reactor, Int. J. Hydrogen Energ. 39 (2014) 3160–3175.

[27] D.H. Vu, K.M. Muttaqi, A.P. Agalgaonkar, A variance inflation factor and backward elimination based robust regression model for forecasting monthly electricity demand using climatic variables, Appl. Energ. 140 (2015) 385–394.

[28] J.T. Carneiro, T.J. Savenije, J.A. Moulijn, G. Mul, Toward a physically sound structure-activity relationship of TiO_2-based photocatalysts, J. Phys. Chem. C 114 (2010) 327–332.

[29] C.B. Almquist, P. Biswas, Role of synthesis method and particle size of nanostructured TiO_2 on its photoactivity, J. Catal. 212 (2002) 145–156.

[30] Minitab, Inc., Interpret all statistics and graphs for two-way ANOVA, https://support.minitab.com/en-us/minitab-express/1/help-and-how-to/modeling-statistics/anova/how-to/two-way-anova/interpret-the-results/all-statistics-and-graphs/#residuals-versus-order (accessed August 27, 2019).

[31] Minitab, Inc., The Anderson-Darling statistic, https://support.minitab.com/en-us/minitab/19/help-and-how-to/statistics/basic-statistics/supporting-topics/normality/the-anderson-darling-statistic/ (accessed August 27, 2019).

[32] A.H. Ang, W.H. Tang, Determination of probability distribution models, in: W.A. Murray (Ed.), Probability concepts in engineering, John Wiley and Sons, Inc., Hoboken, 2006, pp. 296–300.

[33] Minitab, Inc., What are individual desirability and composite desirability?, https://support.minitab.com/en-us/minitab/18/help-and-how-to/modeling-statistics/using-fitted-models/supporting-topics/response-optimization/what-are-individual-desirability-and-composite-desirability/ (accessed August 27, 2019).

[34] Minitab, Inc., All statistics and graphs for response optimizer, https://support.minitab.com/en-us/minitab/18/help-and-how-to/modeling-statistics/using-fitted-models/how-to/response-optimizer/interpret-the-results/all-statistics-and-graphs/ (accessed August 27, 2019).

CHAPTER 5

GENERAL CONCLUSIONS AND RECOMMENDATIONS

This work attempted to optimize the TOC removal efficiency of UV/TiO_2 photocatalytic degradation of black liquor by controlling five factors. In consideration of up to five factors, the whole process of optimization was divided into two phases. The first phase was considered the preliminary study (Chapter 3), during which the black liquor concentration and the TiO_2 concentration were taken as variables to determine a better initial condition with the assistance of a two-level 2^k design. Based on the initial condition of outstanding TOC removal efficiency, the remaining three factors: pH, temperature, and particle size were optimized simultaneously in Chapter 4 by applying a three-factor, three-level BBD.

According to the results in Chapter 3, the optimal set of conditions was 230 mg $TS\cdot L^{-1}$ black liquor and 2 $g\cdot L^{-1}$ TiO_2. Under this optimal condition, the TOC reduction percentage can be as high as $36.2\pm4.0\%$, which is more than twice the lowest TOC reduction percentage under the condition of 460 mg $TS\cdot L^{-1}$ black liquor and 1 $g\cdot L^{-1}$ TiO_2. This result complied with the trend proposed by Shoko et al. [1] that decreasing substrate concentration and increasing catalyst concentration can optimize the photocatalytic performance at a high pH level. The statistical analysis of the 2^k design indicates the significance of the interaction effect between black liquor and TiO_2 concentration on the TOC reduction efficiency. In addition, a high black liquor concentration had a negative effect on the TOC reduction efficiency and dominated the effect on photocatalytic efficiency when only these two factors were considered.

According to the results in Chapter 4, the optimal conditions were a pH of 7.87, 37 ℃, and a catalyst particle size of 5 nm. Under these optimal conditions, the TOC reduction was expected to reach 51.6%, predicted using an RSM quadratic model. ANOVA was performed and indicated that all the linear and square terms were statistically significant, while the interaction terms except for the interaction between pH and temperature were significant. A TiO_2 particle size of 15 nm was not recommended due to a negative effect on TOC reduction. In addition, the optimization of RSM can be proven when compared to the optimum results of Chapter 3 (36.2%), with an additional 15% TOC removal efficiency.

Although the optimal condition of five factors was identified, a more comprehensive optimization can be performed in the future. A wider range of each factor can also be considered, particularly a higher pH and a wider range of temperatures. As the factors' values are examined intensively, the cost of each condition could also be taken into consideration as the second response during optimization. In addition, phenolics are one of the abundant byproducts of photocatalysis, and the phenolics could also be taken into consideration because of their ability to affect the process of bio-degradability when used in conjunction with other elements, such as co-digestion with glucose for biogas production [2].

References

[1] E. Shoko, J.C.D. Costa, E.T. White, Optimization of the reaction rate in the photocatalytic degradation of sodium lignosulfonate in a TiO$_2$ slurry reactor: A multivariate study with response surface analysis, Dev. Chem. Eng. Min. Process. 12 (2004) 475–489.

[2] J.E. Hernandez, R.G.J. Edyvean, Inhibition of biogas production and biodegradability by substituted phenolic compounds in anaerobic sludge, J. Hazard. Mater. 160 (2008) 20–28.

APPENDICES

Chapter 1: copyright

(collectively "WILEY"). By clicking "accept" in connection with completing this licensing transaction, you agree that the following terms and conditions apply to this transaction (along with the billing and payment terms and conditions established by the Copyright Clearance Center Inc., ("CCC's Billing and Payment terms and conditions"), at the time that you opened your RightsLink account (these are available at any time at http://myaccount.copyright.com).

Terms and Conditions

- The materials you have requested permission to reproduce or reuse (the "Wiley Materials") are protected by copyright.

- You are hereby granted a personal, non-exclusive, non-sub licensable (on a stand-alone basis), non-transferable, worldwide, limited license to reproduce the Wiley Materials for the purpose specified in the licensing process. This license, **and any CONTENT (PDF or image file) purchased as part of your order,** is for a one-time use only and limited to any maximum distribution number specified in the license. The first instance of republication or reuse granted by this license must be completed within two years of the date of the grant of this license (although copies prepared before the end date may be distributed thereafter). The Wiley Materials shall not be used in any other manner or for any other purpose, beyond what is granted in the license. Permission is granted subject to an appropriate acknowledgement given to the author, title of the material/book/journal and the publisher. You shall also duplicate the copyright notice that appears in the Wiley publication in your use of the Wiley Material. Permission is also granted on the understanding that nowhere in the text is a previously published source acknowledged for all or part of this Wiley Material. Any third party content is expressly excluded from this permission.

- With respect to the Wiley Materials, all rights are reserved. Except as expressly granted by the terms of the license, no part of the Wiley Materials may be copied, modified, adapted (except for minor reformatting required by the new Publication), translated, reproduced, transferred or distributed, in any form or by any means, and no derivative works may be made based on the Wiley Materials without the prior permission of the respective copyright owner.**For STM Signatory Publishers clearing permission under the terms of the STM Permissions Guidelines only, the terms of the license are extended to include subsequent editions and for editions in other languages, provided such editions are for the work as a whole in situ and does not involve the separate exploitation of the permitted figures or extracts,** You may not alter, remove or suppress in any manner any copyright, trademark or other notices displayed by the Wiley Materials. You may not license, rent, sell, loan, lease, pledge, offer as security, transfer or assign the Wiley Materials on a stand-alone basis, or any of the rights granted to you hereunder to any other person.

- The Wiley Materials and all of the intellectual property rights therein shall at all times remain the exclusive property of John Wiley & Sons Inc, the Wiley Companies, or their respective licensors, and your interest therein is only that of having possession of and the right to reproduce the Wiley Materials pursuant to Section 2 herein during the continuance of this Agreement. You agree that you own no right, title or interest in or to the Wiley Materials or any of the intellectual property rights therein. You shall have no rights hereunder other than the license as provided for above in Section 2. No right, license or interest to any trademark, trade name, service mark or other branding ("Marks") of WILEY or its licensors is granted hereunder, and you agree that you shall not assert any such right, license or interest with respect thereto

- NEITHER WILEY NOR ITS LICENSORS MAKES ANY WARRANTY OR REPRESENTATION OF ANY KIND TO YOU OR ANY THIRD PARTY, EXPRESS, IMPLIED OR STATUTORY, WITH RESPECT TO THE MATERIALS OR THE ACCURACY OF ANY INFORMATION CONTAINED IN THE MATERIALS, INCLUDING, WITHOUT LIMITATION, ANY IMPLIED WARRANTY OF MERCHANTABILITY, ACCURACY, SATISFACTORY QUALITY, FITNESS FOR A PARTICULAR PURPOSE, USABILITY, INTEGRATION OR NON-INFRINGEMENT AND ALL SUCH WARRANTIES ARE HEREBY EXCLUDED BY WILEY AND ITS LICENSORS AND WAIVED BY YOU.

- WILEY shall have the right to terminate this Agreement immediately upon breach of this Agreement by you.

- You shall indemnify, defend and hold harmless WILEY, its Licensors and their respective directors, officers, agents and employees, from and against any actual or threatened claims, demands, causes of action or proceedings arising from any breach of this Agreement by you.

- IN NO EVENT SHALL WILEY OR ITS LICENSORS BE LIABLE TO YOU OR ANY OTHER PARTY OR ANY OTHER PERSON OR ENTITY FOR ANY SPECIAL, CONSEQUENTIAL, INCIDENTAL, INDIRECT, EXEMPLARY OR PUNITIVE DAMAGES, HOWEVER CAUSED, ARISING OUT OF OR IN CONNECTION WITH THE DOWNLOADING, PROVISIONING, VIEWING OR USE OF THE MATERIALS REGARDLESS OF THE FORM OF ACTION, WHETHER FOR BREACH OF CONTRACT, BREACH OF WARRANTY, TORT, NEGLIGENCE, INFRINGEMENT OR OTHERWISE (INCLUDING, WITHOUT LIMITATION, DAMAGES BASED ON LOSS OF PROFITS, DATA, FILES, USE, BUSINESS OPPORTUNITY OR CLAIMS OF THIRD PARTIES), AND WHETHER OR NOT THE PARTY HAS BEEN ADVISED OF THE POSSIBILITY OF SUCH DAMAGES. THIS LIMITATION SHALL APPLY NOTWITHSTANDING ANY FAILURE OF ESSENTIAL PURPOSE OF ANY LIMITED REMEDY PROVIDED HEREIN.

- Should any provision of this Agreement be held by a court of competent jurisdiction to be illegal, invalid, or unenforceable, that provision shall be deemed amended to achieve as nearly as possible the same economic effect as the original provision, and the legality, validity and enforceability of the remaining provisions of this Agreement shall not be affected or impaired thereby.

- The failure of either party to enforce any term or condition of this Agreement shall not constitute a waiver of either party's right to enforce each and every term and condition of this Agreement. No breach under this agreement shall be deemed waived or excused by either party unless such waiver or consent is in writing signed by the party granting such waiver or consent. The waiver by or consent of a party to a breach of any provision of this Agreement shall not operate or be construed as a waiver of or consent to any other or subsequent breach by such other party.

- This Agreement may not be assigned (including by operation of law or otherwise) by you without WILEY's prior written consent.

- Any fee required for this permission shall be non-refundable after thirty (30) days from receipt by the CCC.

- These terms and conditions together with CCC's Billing and Payment terms and conditions (which are incorporated herein) form the entire agreement between you and WILEY concerning this licensing transaction and (in the absence of fraud) supersedes all prior agreements and representations of the parties, oral or written. This Agreement may not be amended except in writing signed by both parties. This Agreement shall be binding upon and inure to the benefit of the parties' successors, legal representatives, and authorized assigns.

- In the event of any conflict between your obligations established by these terms and conditions and those established by CCC's Billing and Payment terms and conditions, these terms and conditions shall prevail.

- WILEY expressly reserves all rights not specifically granted in the combination of (i) the license details provided by you and accepted in the course of this licensing transaction, (ii) these terms and conditions and (iii) CCC's Billing and Payment terms and conditions.

- This Agreement will be void if the Type of Use, Format, Circulation, or Requestor Type was misrepresented during the licensing process.

- This Agreement shall be governed by and construed in accordance with the laws of the State of New York, USA, without regards to such state's conflict of law rules. Any legal action, suit or proceeding arising out of or relating to these Terms and Conditions or the breach thereof shall be instituted in a court of competent jurisdiction in New York County in the State of New York in the United States of America and each party hereby consents and submits to the personal jurisdiction of such court, waives any objection to venue in such court and consents to service of process by registered or certified mail, return receipt requested, at the last known address of such party.

WILEY OPEN ACCESS TERMS AND CONDITIONS
Wiley Publishes Open Access Articles in fully Open Access Journals and in Subscription journals offering Online Open. Although most of the fully Open Access journals publish open access articles under the terms of the Creative Commons Attribution (CC BY) License only, the subscription journals and a few of the Open Access Journals offer a choice of Creative Commons Licenses. The license type is clearly identified on the article.
The Creative Commons Attribution License
The Creative Commons Attribution License (CC-BY) allows users to copy, distribute and transmit an article, adapt the article and make commercial use of the article. The CC-BY license permits commercial and non-
Creative Commons Attribution Non-Commercial License
The Creative Commons Attribution Non-Commercial (CC-BY-NC)License permits use, distribution and reproduction in any medium, provided the original work is properly cited and is not used for commercial purposes.(see below)

Creative Commons Attribution-Non-Commercial-NoDerivs License
The Creative Commons Attribution Non-Commercial-NoDerivs License (CC-BY-NC-ND) permits use, distribution and reproduction in any medium, provided the original work is properly cited, is not used for commercial purposes and no modifications or adaptations are made. (see below)
Use by commercial "for-profit" organizations
Use of Wiley Open Access articles for commercial, promotional, or marketing purposes requires further explicit permission from Wiley and will be subject to a fee.

Further details can be found on Wiley Online Library
http://olabout.wiley.com/WileyCDA/Section/id-410895.html

Other Terms and Conditions:

v1.10 Last updated September 2015

Questions? customercare@copyright.com or +1-855-239-3415 (toll free in the US) or +1-978-646-2777.

This Agreement between 1989 Wyandotte St W ("You") and Elsevier ("Elsevier") consists of your license details and the terms and conditions provided by Elsevier and Copyright Clearance Center.

License Number	4643151236812
License date	Aug 06, 2019
Licensed Content Publisher	Elsevier
Licensed Content Publication	Analytica Chimica Acta
Licensed Content Title	Box-Behnken design: An alternative for the optimization of analytical methods
Licensed Content Author	S.L.C. Ferreira,R.E. Bruns,H.S. Ferreira,G.D. Matos,J.M. David,G.C. Brandão,E.G.P. da Silva,L.A. Portugal,P.S. dos Reis,A.S. Souza,W.N.L. dos Santos
Licensed Content Date	Aug 10, 2007
Licensed Content Volume	597
Licensed Content Issue	2
Licensed Content Pages	8
Start Page	179
End Page	186
Type of Use	reuse in a thesis/dissertation
Intended publisher of new work	other
Portion	figures/tables/illustrations
Number of figures/tables/illustrations	1
Format	both print and electronic
Are you the author of this Elsevier article?	No
Will you be translating?	No
Original figure numbers	Figure 1
Title of your thesis/dissertation	Using TiO2 to Optimize the Photocatalytic Degradation of Kraft Black Liquor Using Response Surface Methodology
Expected completion date	Aug 2019
Estimated size (number of pages)	90
Requestor Location	Zihan 401 Sunset Ave
	Windsor, ON N9B 3P4 Canada Attn: 401 Sunset Ave

Terms and Conditions

INTRODUCTION

1. The publisher for this copyrighted material is Elsevier. By clicking "accept" in connection with completing this licensing transaction, you agree that the following terms and conditions apply to this transaction (along with the Billing and Payment terms and conditions established by Copyright Clearance Center, Inc. ("CCC"), at the time that you opened your Rightslink account and that are available at any time at http://myaccount.copyright.com).

GENERAL TERMS

2. Elsevier hereby grants you permission to reproduce the aforementioned material subject to the terms and conditions indicated.

3. Acknowledgement: If any part of the material to be used (for example, figures) has appeared in our publication with credit or acknowledgement to another source, permission must also be sought from that source. If such permission is not obtained then that material may not be included in your publication/copies. Suitable acknowledgement to the source must be made, either as a footnote or in a reference list at the end of your publication, as follows:

"Reprinted from Publication title, Vol /edition number, Author(s), Title of article / title of chapter, Pages No., Copyright (Year), with permission from Elsevier [OR APPLICABLE SOCIETY COPYRIGHT OWNER]." Also Lancet special credit - "Reprinted from The Lancet, Vol. number, Author(s), Title of article, Pages No., Copyright (Year), with permission from Elsevier."

4. Reproduction of this material is confined to the purpose and/or media for which permission is hereby given.

5. Altering/Modifying Material: Not Permitted. However figures and illustrations may be altered/adapted minimally to serve your work. Any other abbreviations, additions, deletions and/or any other alterations shall be made only with prior written authorization of Elsevier Ltd. (Please contact Elsevier at permissions@elsevier.com). No modifications can be made to any Lancet figures/tables and they must be reproduced in full.

6. If the permission fee for the requested use of our material is waived in this instance, please be advised that your future requests for Elsevier materials may attract a fee.

7. Reservation of Rights: Publisher reserves all rights not specifically granted in the combination of (i) the license details provided by you and accepted in the course of this licensing transaction, (ii) these terms and conditions and (iii) CCC's Billing and Payment terms and conditions.

8. License Contingent Upon Payment: While you may exercise the rights licensed immediately upon issuance of the license at the end of the licensing process for the transaction, provided that you have disclosed complete and accurate details of your proposed use, no license is finally effective unless and until full payment is received from you (either by publisher or by CCC) as provided in CCC's Billing and Payment terms and conditions. If full payment is not received on a timely basis, then any license preliminarily granted shall be deemed automatically revoked and shall be void as if never granted. Further, in the event that you breach any of these terms and conditions or any of CCC's Billing and Payment terms and conditions, the license is automatically revoked and shall be void as if never granted. Use of materials as described in a revoked license, as well as any use of the materials beyond the scope of an unrevoked license, may constitute copyright infringement and publisher reserves the right to take any and all action to protect its copyright in the materials.

9. Warranties: Publisher makes no representations or warranties with respect to the licensed material.

10. Indemnity: You hereby indemnify and agree to hold harmless publisher and CCC, and their respective officers, directors, employees and agents, from and against any and all

claims arising out of your use of the licensed material other than as specifically authorized pursuant to this license.

11. No Transfer of License: This license is personal to you and may not be sublicensed, assigned, or transferred by you to any other person without publisher's written permission.

12. No Amendment Except in Writing: This license may not be amended except in a writing signed by both parties (or, in the case of publisher, by CCC on publisher's behalf).

13. Objection to Contrary Terms: Publisher hereby objects to any terms contained in any purchase order, acknowledgment, check endorsement or other writing prepared by you, which terms are inconsistent with these terms and conditions or CCC's Billing and Payment terms and conditions. These terms and conditions, together with CCC's Billing and Payment terms and conditions (which are incorporated herein), comprise the entire agreement between you and publisher (and CCC) concerning this licensing transaction. In the event of any conflict between your obligations established by these terms and conditions and those established by CCC's Billing and Payment terms and conditions, these terms and conditions shall control.

14. Revocation: Elsevier or Copyright Clearance Center may deny the permissions described in this License at their sole discretion, for any reason or no reason, with a full refund payable to you. Notice of such denial will be made using the contact information provided by you. Failure to receive such notice will not alter or invalidate the denial. In no event will Elsevier or Copyright Clearance Center be responsible or liable for any costs, expenses or damage incurred by you as a result of a denial of your permission request, other than a refund of the amount(s) paid by you to Elsevier and/or Copyright Clearance Center for denied permissions.

LIMITED LICENSE

The following terms and conditions apply only to specific license types:

15. **Translation**: This permission is granted for non-exclusive world **English** rights only unless your license was granted for translation rights. If you licensed translation rights you may only translate this content into the languages you requested. A professional translator must perform all translations and reproduce the content word for word preserving the integrity of the article.

16. **Posting licensed content on any Website**: The following terms and conditions apply as follows: Licensing material from an Elsevier journal: All content posted to the web site must maintain the copyright information line on the bottom of each image; A hyper-text must be included to the Homepage of the journal from which you are licensing at http://www.sciencedirect.com/science/journal/xxxxx or the Elsevier homepage for books at http://www.elsevier.com; Central Storage: This license does not include permission for a scanned version of the material to be stored in a central repository such as that provided by Heron/XanEdu.

Licensing material from an Elsevier book: A hyper-text link must be included to the Elsevier homepage at http://www.elsevier.com . All content posted to the web site must maintain the copyright information line on the bottom of each image.

Posting licensed content on Electronic reserve: In addition to the above the following clauses are applicable: The web site must be password-protected and made available only to bona fide students registered on a relevant course. This permission is granted for 1 year only. You may obtain a new license for future website posting.

17. **For journal authors:** the following clauses are applicable in addition to the above:
Preprints:
A preprint is an author's own write-up of research results and analysis, it has not been peer-reviewed, nor has it had any other value added to it by a publisher (such as formatting, copyright, technical enhancement etc.).

Authors can share their preprints anywhere at any time. Preprints should not be added to or enhanced in any way in order to appear more like, or to substitute for, the final versions of

articles however authors can update their preprints on arXiv or RePEc with their Accepted Author Manuscript (see below).

If accepted for publication, we encourage authors to link from the preprint to their formal publication via its DOI. Millions of researchers have access to the formal publications on ScienceDirect, and so links will help users to find, access, cite and use the best available version. Please note that Cell Press, The Lancet and some society-owned have different preprint policies. Information on these policies is available on the journal homepage.

Accepted Author Manuscripts: An accepted author manuscript is the manuscript of an article that has been accepted for publication and which typically includes author-incorporated changes suggested during submission, peer review and editor-author communications.

Authors can share their accepted author manuscript:

- immediately
    - via their non-commercial person homepage or blog
    - by updating a preprint in arXiv or RePEc with the accepted manuscript
    - via their research institute or institutional repository for internal institutional uses or as part of an invitation-only research collaboration work-group
    - directly by providing copies to their students or to research collaborators for their personal use
    - for private scholarly sharing as part of an invitation-only work group on commercial sites with which Elsevier has an agreement
- After the embargo period
    - via non-commercial hosting platforms such as their institutional repository
    - via commercial sites with which Elsevier has an agreement

In all cases accepted manuscripts should:

- link to the formal publication via its DOI
- bear a CC-BY-NC-ND license - this is easy to do
- if aggregated with other manuscripts, for example in a repository or other site, be shared in alignment with our hosting policy not be added to or enhanced in any way to appear more like, or to substitute for, the published journal article.

Published journal article (JPA): A published journal article (PJA) is the definitive final record of published research that appears or will appear in the journal and embodies all value-adding publishing activities including peer review co-ordination, copy-editing, formatting, (if relevant) pagination and online enrichment.

Policies for sharing publishing journal articles differ for subscription and gold open access articles:

Subscription Articles: If you are an author, please share a link to your article rather than the full-text. Millions of researchers have access to the formal publications on ScienceDirect, and so links will help your users to find, access, cite, and use the best available version. Theses and dissertations which contain embedded PJAs as part of the formal submission can be posted publicly by the awarding institution with DOI links back to the formal publications on ScienceDirect.

If you are affiliated with a library that subscribes to ScienceDirect you have additional private sharing rights for others' research accessed under that agreement. This includes use for classroom teaching and internal training at the institution (including use in course packs and courseware programs), and inclusion of the article for grant funding purposes.

Gold Open Access Articles: May be shared according to the author-selected end-user license and should contain a CrossMark logo, the end user license, and a DOI link to the formal publication on ScienceDirect.

Please refer to Elsevier's posting policy for further information.

18. **For book authors** the following clauses are applicable in addition to the above: Authors are permitted to place a brief summary of their work online only. You are not allowed to download and post the published electronic version of your chapter, nor may you scan the printed edition to create an electronic version. **Posting to a repository:** Authors are permitted to post a summary of their chapter only in their institution's repository.

19. **Thesis/Dissertation**: If your license is for use in a thesis/dissertation your thesis may be submitted to your institution in either print or electronic form. Should your thesis be published commercially, please reapply for permission. These requirements include permission for the Library and Archives of Canada to supply single copies, on demand, of the complete thesis and include permission for Proquest/UMI to supply single copies, on demand, of the complete thesis. Should your thesis be published commercially, please reapply for permission. Theses and dissertations which contain embedded PJAs as part of the formal submission can be posted publicly by the awarding institution with DOI links back to the formal publications on ScienceDirect.

Elsevier Open Access Terms and Conditions

You can publish open access with Elsevier in hundreds of open access journals or in nearly 2000 established subscription journals that support open access publishing. Permitted third party re-use of these open access articles is defined by the author's choice of Creative Commons user license. See our open access license policy for more information.

Terms & Conditions applicable to all Open Access articles published with Elsevier:

Any reuse of the article must not represent the author as endorsing the adaptation of the article nor should the article be modified in such a way as to damage the author's honour or reputation. If any changes have been made, such changes must be clearly indicated.

The author(s) must be appropriately credited and we ask that you include the end user license and a DOI link to the formal publication on ScienceDirect.

If any part of the material to be used (for example, figures) has appeared in our publication with credit or acknowledgement to another source it is the responsibility of the user to ensure their reuse complies with the terms and conditions determined by the rights holder.

Additional Terms & Conditions applicable to each Creative Commons user license:

CC BY: The CC-BY license allows users to copy, to create extracts, abstracts and new works from the Article, to alter and revise the Article and to make commercial use of the Article (including reuse and/or resale of the Article by commercial entities), provided the user gives appropriate credit (with a link to the formal publication through the relevant DOI), provides a link to the license, indicates if changes were made and the licensor is not represented as endorsing the use made of the work. The full details of the license are available at http://creativecommons.org/licenses/by/4.0.

CC BY NC SA: The CC BY-NC-SA license allows users to copy, to create extracts, abstracts and new works from the Article, to alter and revise the Article, provided this is not done for commercial purposes, and that the user gives appropriate credit (with a link to the formal publication through the relevant DOI), provides a link to the license, indicates if changes were made and the licensor is not represented as endorsing the use made of the work. Further, any new works must be made available on the same conditions. The full details of the license are available at http://creativecommons.org/licenses/by-nc-sa/4.0.

CC BY NC ND: The CC BY-NC-ND license allows users to copy and distribute the Article, provided this is not done for commercial purposes and further does not permit distribution of the Article if it is changed or edited in any way, and provided the user gives appropriate credit (with a link to the formal publication through the relevant DOI), provides a link to the license, and that the licensor is not represented as endorsing the use made of the work. The full details of the license are available at http://creativecommons.org/licenses/by-nc-nd/4.0.

Any commercial reuse of Open Access articles published with a CC BY NC SA or CC BY NC ND license requires permission from Elsevier and will be subject to a fee. Commercial reuse includes:

- Associating advertising with the full text of the Article
- Charging fees for document delivery or access
- Article aggregation
- Systematic distribution via e-mail lists or share buttons

Posting or linking by commercial companies for use by customers of those companies.

20. **Other Conditions**:

v1.9

Questions? customercare@copyright.com or +1-855-239-3415 (toll free in the US) or +1-978-646-2777.

List of steps for TS and VS measurements:

1. Wash crucibles, and putting them at 550 ℃ overnight in a muffle furnace
2. Place crucibles into the desiccator for cooling down
3. Measure the weight of graduated cylinder
4. Bring sample (black liquor bottle) in room temperature before analysis
5. Stir the sample adequately
6. Pipette sample from the black liquor bottle
7. Deliver sample to the graduated cylinder up to 3 mL. Rinse the pipette if there is visible residue in it.
8. Measure the total weight of the graduated cylinder containing 3 mL sample
9. Measure the weight of crucible (empty mass)
10. Pour the sample into the crucible from graduated cylinder
11. Rinse the graduated cylinder couple times, and pouring the rinsed liquid into the crucible
12. Place the crucible into the 105 ℃ oven overnight
13. Place the crucible into the desiccator for cooling down
14. Measure the total weight (mass 105 ℃) of crucible + $residue_1$
15. Turn on the muffle furnace up to 550 ℃
16. Place the crucible into the muffle furnace for 2 hours
17. Place crucible into the desiccator for cooling down
18. Measure the total weight (mass 550 ℃) of crucible + $residue_2$ until constant weight
19. Turn off the muffle furnace

All TS and VS measurement were in triplicate.

References:

- TAPPI/ANSI T 650 om-15
- METHOD 1684

Calculations for TS and VS:

$$\text{Total solids} = \text{TS}\left(\frac{mg}{L}\right) = \frac{mass\ 105\ ^{\circ}C\ (g) - empty\ mass\ (g)}{volume\ (mL)} \times 10^6$$

$$\text{Volatile solids} = \text{VS}\left(\frac{mg}{L}\right) = \frac{mass\ 105\ ^{\circ}C\ (g) - mass\ 550\ ^{\circ}C\ (g)}{volume\ (mL)} \times 10^6$$

Empty mass (g) = weight of crucible

Volume (mL) = amount of black liquor added to the crucible

Mass 105 °C (g) = weight of dried residue after 20 hours (to make sure all water is driven off samples) in 105 °C oven and cooling + crucible

Mass 550 °C (g) = weight of dried residue after 2 hours in 550 °C muffle furnace and cooling + crucible

Data:

Empty mass(g)	Volume (mL)	Mass 105 °C (g)	Mass 550 °C (g)
41.6632	3.00	43.4366	42.9159
43.3360	3.00	45.0827	44.5371
43.5366	3.00	45.2823	44.7552

Note: All TS and VS measurements were conducted in triplicate.

Sample calculation:

$$\text{TS} = \frac{43.4366g - 41.6632g}{3.00mL} \times \frac{10^3 mg}{g} \times \frac{10^3 mL}{L} = 591133\left(\frac{mg}{L}\right)$$

$$\text{VS} = \frac{43.4366g - 42.9159g}{3.00mL} \times \frac{10^3 mg}{g} \times \frac{10^3 mL}{L} = 173567\left(\frac{mg}{L}\right)$$

In this study, the TS of black liquor is equal to 585089 ± 1950 mg TS·L^{-1}, which is 585.1 ± 2.0 g TS·L^{-1} on average. The VS of black liquor volatile solids is equal to 177044 ± 584 mg VS·L^{-1}, which is 177.0 ± 0.6 g TS·L^{-1} on average.

Diluting 0.50 g (0.39 mL) black liquor into 1.0 L solution, the TS and VS were calculated as:

$$\text{TS} = 585.1\frac{g}{L} \times \frac{10^3 mg}{g} \times \frac{0.39mL}{1000mL} = 230\left(\frac{mg}{L}\right)$$

$$\text{VS} = 177.0\frac{g}{L} \times \frac{10^3 mg}{g} \times \frac{0.39mL}{1000mL} = 69\left(\frac{mg}{L}\right)$$

VITA AUCTORIS

NAME:	Zihan Wang
PLACE OF BIRTH:	Tianjin, China
YEAR OF BIRTH:	1994
EDUCATION:	Xinhua High School, Tianjin, China, 2012
	Hunan University, B.Sc., Changsha, Hunan, China, 2016
	University of Windsor, M.A.Sc., Windsor, Ontario, 2019